Eur. Phys. J. C (2025) 85:168
https://doi.org/10.1140/epjc/s10052-024-13723-4

THE EUROPEAN PHYSICAL JOURNAL C

Regular Article - Theoretical Physics

Higgs mass predictions in the CP-violating high-scale NMSSM

Christoph Borschensky[1,a], **Thi Nhung Dao**[2,b], **Martin Gabelmann**[3,c], **Margarete Mühlleitner**[1,d], **Heidi Rzehak**[4,e]

[1] Institute for Theoretical Physics, Karlsruhe Institute of Technology, Wolfgang-Gaede-Str. 1, 76131 Karlsruhe, Germany
[2] Phenikaa Institute for Advanced Study, PHENIKAA University, Hanoi 12116, Vietnam
[3] Deutsches Elektronen-Synchrotron DESY, Notkestr. 85, 22607 Hamburg, Germany
[4] Physikalisches Institut, Albert-Ludwigs-Universität Freiburg, Hermann-Herder-Str. 3, 79104 Freiburg, Germany

Received: 10 July 2024 / Accepted: 20 December 2024

Abstract In a supersymmetric theory, large mass hierarchies can lead to large uncertainties in fixed-order calculations of the Standard Model (SM)-like Higgs mass. A reliable prediction is then obtained by performing the calculation in an effective field theory (EFT) framework, involving a matching to the full supersymmetric theory at the high scale to include contributions from the heavy particles, and a subsequent renormalisation-group running down to the low scale. We report on the prediction of the SM-like Higgs mass within the CP-violating next-to-minimal supersymmetric extension of the SM (NMSSM) in a scenario where all non-SM particles feature TeV-scale masses. The matching conditions are calculated at full one-loop order using two approaches. These are the matching of the quartic Higgs couplings as well as of the SM-like Higgs pole masses of the low- and high-scale theory. A comparison between the two methods allows us to estimate the size of terms suppressed by the heavy mass scale that are neglected in a pure EFT calculation as given by the quartic-coupling matching. Furthermore, we study the different sources of uncertainty which enter our calculation as well as the effect of CP-violating phases on the Higgs mass prediction. The matching calculation is implemented in a new version of the public program package `NMSSMCALC`.

Contents

[a] e-mail: christoph.borschensky@kit.edu
[b] e-mail: nhung.daothi@phenikaa-uni.edu.vn (corresponding author)
[c] e-mail: martin.gabelmann@desy.de
[d] e-mail: margarete.muehlleitner@kit.edu
[e] e-mail: heidi.rzehak@physik.uni-freiburg.de

1 Introduction

Since the discovery of the Standard Model Higgs boson with a mass of about 125 GeV by the ATLAS [1] and the CMS collaboration [2] at the large hadron collider (LHC) at CERN, there has been no clear indication of new degrees of freedom in the range of the weak scale (which can be identified with energy scales around the mass of the W boson, $\sim M_W$) to a few TeV scale. Taking into account the constraints from the Higgs data and experimental searches for new degrees of freedom, the parameter space of each Standard Model

Published online: 10 February 2025

extension (SM) should be reinvestigated in terms of whether these models can still satisfy the experimental constraints and give possibly detectable new physics signals. Among them, the minimal supersymmetric extension of the SM (MSSM) is one of the most studied ones. By imposing a symmetry between bosonic and fermionic degrees of freedom, the particle content is more than doubled with respect to the SM. An interesting feature of this model is related to the Higgs sector. It contains two Higgs doublets due to the requirement of the cancellation of gauge anomalies on the one hand as well as for the generation of non-vanishing masses for all quarks on the other hand. Furthermore, the quartic couplings in the Higgs sector are completely determined by the gauge and Yukawa couplings. As a consequence, the Higgs boson masses can be predicted and one of the Higgs boson masses has an upper limit of about 140 GeV including higher-order corrections [3]. This Higgs boson can be identified with the discovered scalar particle. Similar features occur also in the next-to-MSSM (NMSSM), an extension of the MSSM that includes an extra Higgs singlet superfield. However, the upper mass bound can be shifted to higher values due to extra contributions from the Higgs singlet-doublet coupling [4–8].

Three approaches for the computation of the Higgs boson masses including higher-order corrections have been used. These are the fixed-order (FO), the effective field theory (EFT), and the hybrid technique. For the first one, we have to compute Higgs boson self-energies at fixed loop order and diagonalize the loop-corrected Higgs mass matrix. This calculation involves the full particle spectrum and couplings in the broken phase of the electroweak (EW) symmetry of the model. The corrections will contain terms which are proportional to $\ln \tilde{M}_x^2/M_x^2$ [3], where M_x and $\tilde{M}_x$ are a masses of an SM particle x and its superpartner, respectively. These terms are particularly important for the top/stop sector, since the top Yukawa coupling is the largest Yukawa coupling. Therefore, if there is large hierarchy between the stop and the top mass the FO calculation breaks down. In such a case, one needs to resum these large logarithms to obtain reliable results. In the EFT calculation, the couplings of the high-energy extension of the SM are matched to the corresponding ones in the effective low-energy field theory such that at the matching scale the physics described by the two models is the same. If only the SM-like particles of the SM extension are light and all the Beyond-SM (BSM) particles are heavy, then the SM is a suitable EFT. In this case, the loop-corrected SM quartic Higgs coupling at the matching scale can be identified with a loop-corrected BSM quartic Higgs coupling at the same scale. All SM-type contributions proportional to powers of $\ln Q_{\text{match}}^2/M_x^2$ are cancelled out, where Q_{match} is the matching scale. The running SM quartic Higgs coupling is now defined from the BSM quartic Higgs coupling which contains logarithmic terms of the form $\ln \tilde{M}_x^2/Q_{\text{match}}^2$. Then the logarithmic terms become small when $\tilde{M}_x$ is close to Q_{match}. The remaining dependence on $\ln Q_{\text{match}}^2/M_x^2$ can be resummed with the help of the SM renormalisation group equations (RGEs) for the quartic Higgs coupling. In the literature, there exist two ways to match the loop-corrected BSM quartic Higgs coupling. The first one is called quartic coupling matching which is based on the computation of loop corrections to the four-point vertex using the spectrum and couplings in the limit of the unbroken EW symmetry, $v \to 0$, with v being the vacuum expectation value. The second one is called pole-mass matching which is based on the assumption that also in the BSM theory the SM-like quartic Higgs coupling has a relation with the SM-like Higgs pole mass. By computing the BSM contribution to the SM-like Higgs mass, we can extract information on the quartic Higgs coupling. The computation needs to be done in the broken EW symmetry phase and leads to contributions of $\mathcal{O}(v^2/\tilde{M}_x^2)$. The third approach is called the hybrid technique which combines fixed-order calculations with the EFT approach where the leading and next-to-leading logarithms are resummed and care is taken that no double counting occurs. The gain is two-fold. On the one hand, the theory uncertainty at high supersymmetric (SUSY) masses is reduced in comparison to a pure fixed-order result [3]. On the other hand, $\mathcal{O}(v^2/\tilde{M}_x^2)$ effects are taken into account in comparison to the pure EFT approach, where they are integrated out.

A lot of effort has been devoted to the precise calculation of the Higgs boson masses in the NMSSM using fixed-order calculations. Leading one-loop, full one-loop and leading two-loop contributions were presented in [9–27] where the $\overline{\text{DR}}$ renormalisation scheme was applied, except for [19], which also applied a mixed $\overline{\text{DR}}$-on-shell (OS) renormalisation scheme. At two-loop level, all contributions have been computed in the gaugeless limit and using the zero external momentum approximation. The QCD corrections have been discussed in [17] and $\mathcal{O}((\alpha_\lambda + \alpha_\kappa + \alpha_t)^2)$ corrections in [28]. Our group has also contributed to the progress of precision predictions for the masses. The full one-loop corrections with momentum dependence were presented in [29,30] and the two-loop corrections of $\mathcal{O}(\alpha_t\alpha_s)$ in [31], of $\mathcal{O}(\alpha_t^2)$ in [32], and of $\mathcal{O}((\alpha_t + \alpha_\lambda + \alpha_\kappa)^2)$ in [33] for both the CP-conserving and the CP-violating NMSSM. We were the first ones to apply a mixed $\overline{\text{DR}}$-OS scheme in the NMSSM with the possibility to choose between either $\overline{\text{DR}}$ or OS conditions in the renormalisation scheme for the top/stop sector. We implemented our FO calculations at one-loop and two-loop $\mathcal{O}(\alpha_t\alpha_s)$, $\mathcal{O}(\alpha_t^2)$, and $\mathcal{O}((\alpha_t + \alpha_\lambda + \alpha_\kappa)^2)$ level in the program package `NMSSMCALC` [34] which also computes the Higgs boson decay widths and branching ratios both for the CP-conserving and CP-violating case. The code furthermore includes the computation of the loop-corrected trilinear Higgs self-couplings at one-loop [35] and at two-loop $\mathcal{O}(\alpha_t\alpha_s)$ [36] and $\mathcal{O}(\alpha_t^2)$ [37] as well as the loop cor-

rections to the ρ parameter and the W boson mass [38]. There are also other public codes such as NMSSMTools [39,40], SARAH/SPheno [41–46], SOFTSUSY [47,48], FlexibleSUSY [49,50] which are dedicated to the computation of the NMSSM spectrum, decay widths and other observables.

There have been much less activities regarding the EFT approach in the precision Higgs mass calculation in the NMSSM. A discussion of EFT in generic SUSY models including also the NMSSM has been presented in [51]. There the loop-corrected quartic Higgs coupling is obtained from the loop-corrected mass of the lightest Higgs boson after subtracting the corresponding part of the SM. This matching condition has been implemented in FlexibleEFTHiggs and later in SARAH/SPheno [52]. In Ref. [53], the authors have used the matching condition where the loop-corrected quartic Higgs coupling is obtained from the loop-corrected four-point vertex. They have combined a full one-loop computation with the QCD two-loop contributions for the quartic Higgs coupling. This computation has been performed in the limit of the unbroken EW symmetry where the Higgs doublet vacuum expectation values $v_u, v_d \to 0$ while the singlet vacuum expectation value v_s is kept non-vanishing and large so that the singlet Higgs masses are very heavy and can then be integrated out.

Our purpose in this paper is threefold. First, we implement both matching conditions discussed in Refs. [51] and [53]. For the pole-mass matching condition we make use of our FO computations of the full one-loop corrections to the Higgs boson masses, which have been implemented in our computer code NMSSMCALC. For this, we modify the renormalisation scheme from the mixed OS-$\overline{\text{DR}}$ to a pure $\overline{\text{DR}}$ scheme for all parameters except the tadpoles for which we still make use of OS-like conditions as in the previously used mixed OS-$\overline{\text{DR}}$ scheme. Using $\overline{\text{DR}}$/$\overline{\text{MS}}$ quantities conveniently enables us to make use of higher-order results in the renormalisation group evolution from the literature. For the four-point vertex matching condition, we compute the full one-loop corrections in the limit of the unbroken phase of the EW symmetry in the $\overline{\text{DR}}$ scheme and discuss subtleties related to the $v \to 0$ limit and finite tadpole corrections. We then compare the effect of the two matching methods on the Higgs mass prediction in a large region of the parameter space where the scale of the SUSY particle masses ranges from TeV to hundred TeV. We also compare the EFT approach and the FO calculation in the mixed OS-$\overline{\text{DR}}$ scheme being available in NMSSMCALC where the renormalisation scale is chosen to be the matching scale in the EFT approach. Second, we discuss the effect of the CP-violating phases in the EFT approach which has not been done in the previous publications. Third, we provide an updated version of NMSSMCALC that gives a better treatment in the case where a large mass hierarchy between BSM and SM-like particles occurs.

The paper is organized as follows. In Sect. 2 we introduce the NMSSM, set up the notation and derive expressions for the tree-level mass matrices and transformations into the mass basis in the limit of a vanishing electroweak VEV. Section 3 discusses the general ingredients for a Higgs mass calculation using an EFT approach. In the first two subsections the quartic-coupling and pole-mass matching approaches are explained in detail while the third subsection describes the estimate of theoretical uncertainties. Section 4 is dedicated to the numerical analysis which validates our results numerically with results from the literature and studies the different EFT approaches and their uncertainties as well as compares to the FO calculation. We conclude in Sect. 5. The appendix contains the derivation of the tadpole-expansion around a small VEV and details on the implementation in the program NMSSMCALC.

2 The high-scale NMSSM at tree-level

We briefly review the basic ingredients of the complex NMSSM to set up our notation for later use. The model is specified by a scale invariant superpotential $\mathcal{W}_{\text{NMSSM}}$,

$$\mathcal{W}_{\text{NMSSM}} = \left[y_e \hat{H}_d \cdot \hat{L} \hat{E}^c + y_d \hat{H}_d \cdot \hat{Q} \hat{D}^c - y_u \hat{H}_u \hat{Q} \hat{U}^c \right] - \lambda \hat{S} \hat{H}_d \cdot \hat{H}_u + \frac{1}{3} \kappa \hat{S}^3 \,, \tag{2.1}$$

where $\hat{H}_d$ and $\hat{H}_u$ are the Higgs doublet superfields, $\hat{S}$ the Higgs singlet superfield and $\hat{L}$, $\hat{Q}$, as well as $\hat{E}$, $\hat{D}$, and $\hat{U}$ the left-handed lepton and quark doublet superfields as well as the right-handed lepton, down-type, and up-type quark singlet superfields, respectively. In the following, we will denote the scalar part of the Higgs superfields and the fermion part of the lepton and quark superfields with the same letter without a hat. The lepton, down-type, and up-type quark Yukawa couplings are y_e, y_d, y_u which are 3×3 matrices that we assume to be diagonal. The summation over generation indices is implicit. The coupling between the Higgs doublet and Higgs singlet superfields is governed by λ and the Higgs singlet superfield self-coupling is κ. Both λ, κ are considered to be complex parameters with corresponding phases $\varphi_\lambda, \varphi_\kappa$. All Yukawas couplings are taken to be real by rephasing the left- and right-handed Weyl-spinor fields accordingly. The soft-SUSY breaking Lagrangian comprises the soft-SUSY breaking parameters,

$$\begin{aligned}\mathcal{L}_{\text{soft, NMSSM}} = & -m_{H_d}^2 H_d^\dagger H_d - m_{H_u}^2 H_u^\dagger H_u - m_{\tilde{Q}}^2 \tilde{Q}^\dagger \tilde{Q} \\ & - m_{\tilde{L}}^2 \tilde{L}^\dagger \tilde{L} - m_{\tilde{u}_R}^2 \tilde{u}_R^* \tilde{u}_R - m_{\tilde{d}_R}^2 \tilde{d}_R^* \tilde{d}_R \\ & - m_{\tilde{e}_R}^2 \tilde{e}_R^* \tilde{e}_R - (\epsilon_{ij} [y_e A_e H_d^i \tilde{L}^j \tilde{e}_R^* + y_d A_d H_d^i \tilde{Q}^j \tilde{d}_R^* \\ & - y_u A_u H_u^i \tilde{Q}^j \tilde{u}_R^*] + \text{h.c.})\end{aligned}$$

$$-\frac{1}{2}(M_1\tilde{B}\tilde{B}+M_2\tilde{W}_i\tilde{W}_i+M_3\tilde{G}\tilde{G}+\text{h.c.})$$
$$-m_S^2|S|^2+(\epsilon_{ij}\lambda A_\lambda S H_d^i H_u^j-\frac{1}{3}\kappa A_\kappa S^3+\text{h.c.}), \quad (2.2)$$

where $\tilde{B}$, $\tilde{W}_i$, $\tilde{G}$ are the fermionic $U(1)$ bino, $SU(2)$ wino and $SU(3)$ gluino fields and A_e, A_d, A_u are the soft-SUSY-breaking trilinear couplings, which are 3×3 matrices and assumed to be diagonal in this paper; again, the summation over the generation indices is implicit here. The soft-SUSY-breaking mass parameters of the sfermions and Higgs fields, $m^2_{\tilde{Q}}$, $m^2_{\tilde{L}}$, $m^2_{\tilde{u}_R}$, $m^2_{\tilde{d}_R}$, $m^2_{\tilde{e}_R}$, $m^2_{H_d}$, $m^2_{H_u}$, and m^2_S are real and positive while the gaugino masses M_1, M_2, M_3 and the soft SUSY breaking trilinear couplings are complex in general. The scalar Higgs potential is obtained from the superpotential in (2.1), the soft-SUSY breaking part of the Lagrangian (2.2) and the D terms originating from the gauge sector of the Lagrangian. Requiring the scalar potential to be minimal at non-vanishing vacuum expectation values (VEVs) of the two Higgs doublets leads to spontaneous breaking of the EW gauge symmetry. Allowing also for the possibility of a singlet VEV, the three Higgs boson fields can be expanded about their VEVs v_u, v_d, and v_s, respectively, as

$$H_d=\begin{pmatrix}\frac{v_d+h_d+ia_d}{\sqrt{2}}\\ h_d^-\end{pmatrix},\quad H_u=e^{i\varphi_u}\begin{pmatrix}h_u^+\\ \frac{v_u+h_u+ia_u}{\sqrt{2}}\end{pmatrix},$$
$$S=\frac{e^{i\varphi_s}}{\sqrt{2}}(v_s+h_s+ia_s)\,, \quad (2.3)$$

with the CP-violating phases $\varphi_{u,s}$.

For a more comprehensive introduction of the model and its mass spectrum of all sectors at tree-level in the broken phase we refer the reader to our paper [54]. We follow the same convention as in [54].

Since for the quartic coupling matching we need expressions for masses and mixings in the unbroken phase of the EW symmetry, in the following, we present the spectrum of the model in the limit $v_u, v_d \to 0$ but with a fixed ratio of the two VEVs,

$$\tan\beta=\frac{v_u}{v_d}, \quad (2.4)$$

and a non-vanishing singlet VEV v_s. We denote the SM-like VEV as v, which is related to the two Higgs doublet VEVs as

$$v^2=v_u^2+v_d^2. \quad (2.5)$$

Higgs Bosons In the limit $v\to 0$ the mass matrices of the CP-violating NMSSM take a particularly simple form which allows for an analytical diagonalisation. First, we solve the tadpole equations of t_{h_u}, t_{h_d}, t_{h_s} and t_{a_d}, t_{a_s} for the soft-SUSY breaking squared masses $m^2_{H_u}, m^2_{H_d}, m^2_S$ and the imaginary parts of the parameters A_λ, A_κ, see e.g. Ref. [32]. This is done without taking the limit $v\to 0$ since the solution to the tadpoles may contain terms $\mathcal{O}(v^{-n})$ which are multiplied with terms $\mathcal{O}(v^{+m})$ when inserting them into the mass matrices.[1]

Using the tree-level tadpole solutions in the tree-level mass matrices and then performing the limit $v\to 0$, we obtain the following: The squared mass matrix of the charged Higgs boson has one vanishing eigenvalue corresponding to the Goldstone boson and one non-zero eigenvalue corresponding to the physical charged Higgs boson,[2]

$$m^2_{G^\pm}=0 \quad (2.6a)$$
$$m^2_{H^\pm}=\frac{|\lambda|(1+\tan^2\beta)v_s}{2\tan\beta\cos(\varphi_w-\varphi_y)}\left(\sqrt{2}\text{Re}A_\lambda+|\kappa|v_s\cos\varphi_w\right), \quad (2.6b)$$

where

$$\varphi_w=3\varphi_s+\varphi_\kappa \quad (2.7)$$
$$\varphi_y=2\varphi_s+\varphi_\kappa-\varphi_\lambda-\varphi_u. \quad (2.8)$$

Thus, we can trade $\text{Re}A_\lambda$ for $m^2_{H^\pm}$. The squared mass matrix for the neutral Higgs bosons takes a block-diagonal form where, after the use of the tadpole solutions, neither the CP-even and the CP-odd components nor the doublet and singlet components mix. The mixing matrix which diagonalizes the neutral Higgs mass matrix transforming the basis $(h_d, h_u, h_s, a_d, a_u, a_s)^T$ to the basis (h, H, S, G^0, A, A_s), reads

$$\mathcal{R}(\beta)=\begin{pmatrix}\mathcal{R}^H(\beta) & \mathbf{0}\\ \mathbf{0} & \mathcal{R}^G(\beta)\end{pmatrix} \quad (2.9)$$

with

$$\mathcal{R}^H(\beta)=\begin{pmatrix}c_\beta & s_\beta & 0\\ -s_\beta & c_\beta & 0\\ 0 & 0 & 1\end{pmatrix},\quad \mathcal{R}^G(\beta)=\begin{pmatrix}-c_\beta & s_\beta & 0\\ s_\beta & c_\beta & 0\\ 0 & 0 & 1\end{pmatrix}, \quad (2.10)$$

Diagonalizing the neutral Higgs mass matrix with the help of the mixing matrix in (2.9) results in a diagonal matrix with the entries

$$m^2_h(=m^2_{h_u})=0 \quad (2.11a)$$
$$m^2_H(=m^2_{h_d})=m^2_{H^\pm} \quad (2.11b)$$
$$m^2_{H_s}(=m^2_{h_s})=\frac{|\kappa|v_s(4|\kappa|v_s+\sqrt{2}\frac{\text{Re}A_\kappa}{\cos\varphi_w})}{2} \quad (2.11c)$$

[1] Note that this procedure differs from the one discussed in e.g. [53,55] which only relies on the use of tadpole equations for the singlet BSM fields. We, however, have found very good agreement with [53] in the CP-conserving case, *cf.* Sect. 4.3 and also the discussion in Sect. 3.1.2. This suggests that while the intermediate results differ, the final finite result of the matching condition remains unchanged.

[2] We use small letters m to denote tree-level masses and capital letters M to denote loop-corrected or on-shell input masses.

$$m^2_{G^0}(= m^2_{a_u}) = 0 \tag{2.11d}$$

$$m^2_A(= m^2_{a_d}) = m^2_{H^\pm} \tag{2.11e}$$

$$m^2_{A_s}\,(= m^2_{a_s}) = -\frac{3|\kappa|\mathrm{Re}A_\kappa v_s}{\sqrt{2}\cos\varphi_w}\,. \tag{2.11f}$$

The masses in parenthesis denote the dominant gauge-eigenstates masses. It turns out that for the parameter points that are compatible with all applied constraints and that we discuss in our numerical analysis, the h (H) is mostly h_u-like (h_d-like) and the A (G^0) is mostly a_d-like (a_u-like). The two vanishing eigenvalues correspond to the neutral Goldstone boson and the SM-like Higgs boson mass. These are the only two neutral scalar states that belong to the EFT, and all remaining heavy neutral Higgs bosons are integrated out. The third eigenvalue $m^2_{H_s}$ corresponds to the mass of the scalar singlet. The second and fifth eigenvalues, m^2_H and m^2_A, are degenerate and coincide with the mass of the charged Higgs boson, $m^2_{H^\pm}$. The last eigenvalue, $m^2_{A_s}$, corresponds to the pseudoscalar singlet.

Fermions Using the approximation $v \to 0$ the top quark as well as all other SM fermions are massless and do not mix with each other. Considering the fermionic supersymmetric partner particles and assuming the Weyl basis $\psi^0 = (\tilde{B}, \tilde{W}_3, \tilde{H}^0_d, \tilde{H}^0_u, \tilde{S})^T$ and $\psi^- = (\tilde{W}^-, \tilde{H}^-_u)^T$ where $\tilde{H}^0_d$, $\tilde{H}^0_u$, $\tilde{H}^-_u$, $\tilde{S}$ are the neutral and charged doublet Higgsino and singlino fields, respectively, for the neutral and the charged fields results in the following neutralino and chargino mass matrices,

$$M_N = \begin{pmatrix} M_1 & 0 & 0 & 0 & 0 \\ 0 & M_2 & 0 & 0 & 0 \\ 0 & 0 & 0 & -\lambda\frac{v_s}{\sqrt{2}}e^{i\varphi_s} & 0 \\ 0 & 0 & -\lambda\frac{v_s}{\sqrt{2}}e^{i\varphi_s} & 0 & 0 \\ 0 & 0 & 0 & 0 & \sqrt{2}\kappa v_s e^{i\varphi_s} \end{pmatrix}$$

$$M_C = \begin{pmatrix} M_2 & 0 \\ 0 & \lambda\frac{v_s}{\sqrt{2}}e^{i\varphi_s} \end{pmatrix}. \tag{2.12}$$

The neutralinos and charginos have a non-zero mass. Their mass-matrices can be diagonalized analytically. We find the following mass eigenvalues:

$$m_{\chi^0_1} = |M_1| \tag{2.13a}$$

$$m_{\chi^0_2} = |M_2| \tag{2.13b}$$

$$m_{\chi^0_3} = m_{\chi^\pm_2} \tag{2.13c}$$

$$m_{\chi^0_4} = m_{\chi^\pm_2} \tag{2.13d}$$

$$m_{\chi^0_5} = \sqrt{m^2_{A_s}/3 + m^2_{H_s}} \tag{2.13e}$$

$$m_{\chi^\pm_1} = |M_2| \tag{2.13f}$$

$$m_{\chi^\pm_2} = \frac{|\lambda|}{|\kappa|}\frac{\sqrt{m^2_{A_s}/3 + m^2_{H_s}}}{2}\,, \tag{2.13g}$$

where all complex phases have been absorbed into the rotation matrices and v_s is replaced by

$$v_s = \frac{\sqrt{m^2_{A_s}/3 + m^2_{H_s}}}{\sqrt{2}|\kappa|}. \tag{2.14}$$

Sfermions In the limit $v \to 0$ the squared sfermion mass matrices are only given in terms of the soft-SUSY breaking parameters, and the mixing between left- and right-handed scalars vanishes. Thus their interaction eigenstates coincide with the mass eigenstates,

$$m^2_{\tilde{X}} = \begin{pmatrix} \boldsymbol{m}^2_{\tilde{X}_L} & 0 \\ 0 & \boldsymbol{m}^2_{\tilde{X}_R} \end{pmatrix}, \qquad X = u, d, l\,, \tag{2.15}$$

assuming minimal flavour violation (i.e. diagonal $\boldsymbol{m}^2_{\tilde{X}_L}$, $\boldsymbol{m}^2_{\tilde{X}_R}$). The above diagonal mass matrix has two eigenstates $\tilde{X}_{1,2}$ with masses $m_{\tilde{X}_{1,2}} = \{m_{\tilde{X}_L}, m_{\tilde{X}_R}\}$ for the superpartners of each SM fermion generation. Note that only the 3rd generation of quarks and leptons has significant effects on the Higgs boson masses.

3 The loop-corrected Higgs mass in the EFT approach

In the scenario that we are considering in this paper, all the soft-SUSY-breaking mass parameters of the sfermions and gauginos, $m^2_{\tilde{Q}}$, $m^2_{\tilde{L}}$, $m^2_{\tilde{u}_R}$, $m^2_{\tilde{d}_R}$, $m^2_{\tilde{e}_R}$, and M_1, M_2, M_3, together with $m_{H_s}, m_{A_s}, m_{H^\pm}$ are much larger than the SM EW scale. These masses are similar to $\sim M_{\rm SUSY}$ where $M_{\rm SUSY} \gg v$. Since all SM-like particles have a mass $m_{\rm SM} \propto v$, this means $M_{\rm SUSY} \gg m_{\rm SM}$.

In such a scenario, a fixed-order approach will lead to large logarithms of $\ln(v^2/M^2_{\rm SUSY})$ which will destroy the perturbative expansion and hence a precise prediction. Therefore, we follow the EFT approach where we match the NMSSM to the effective field theory (that we identify with the SM in this paper) at the scale $M_{\rm SUSY}$ in such a way that at $M_{\rm SUSY}$ both theories lead to the same physical predictions. The contributions containing large logarithms of $\ln(v^2/M^2_{\rm SUSY})$ will be resummed through the SM renormalisation group equations (RGE). In the NMSSM calculation, we will denote the SM-like Higgs that is matched to the Higgs boson of the EFT as the one which is predominantly made up of the h_u component of (2.3).

For the matching procedure, we are following two matching condition schemes which allow us to relate the effective

quartic Higgs coupling $\lambda_h^{\rm SM}$ in the SM[3] to the one in the NMSSM. For the quartic interaction term we use the normalisation $-\lambda_h^{\rm SM}|H|^4$, with the neutral component of the SM Higgs doublet H given by $H^0 = \frac{1}{\sqrt{2}}(v^{\rm SM} + h + iG^0)$.

- In the first scheme, we directly require the four-point functions, i.e. matrix elements, with four external Higgs bosons in the SM and the SM-like Higgs bosons in the NMSSM to be the same at the matching scale. We can then calculate loop corrections to the quartic Higgs coupling within the NMSSM, $\lambda_h^{\rm NMSSM}$, that we then identify with the loop-corrected SM one $\lambda_h^{\rm SM}$. In the following, we will refer to this scheme as *quartic-coupling matching*.
- In the second scheme, we demand that the pole masses of the Higgs boson in the SM and the SM-like Higgs boson in the NMSSM are equal at the matching scale. The SM $\overline{\rm MS}$ mass at the matching scale is then computed from this matching condition. Here, it has to be ensured that all large logarithms of $\ln(v^2/M_{\rm SUSY}^2)$ are canceled by applying a proper expansion. The extraction of the effective quartic Higgs coupling via (3.29) is discussed in Sect. 3.2 in more detail. We will refer to this scheme as *pole-mass matching*.

The major difference between the two matching schemes consists in the diagrams to be evaluated (*cf.* [56] for a detailed discussion): While the quartic-coupling matching requires four-point functions to be calculated in the limit of $v \to 0$, the pole-mass matching requires at most only two-point functions, i.e. self energies, to be evaluated, at the expense of having to carry out the calculation in the EW-broken phase and then expanding systematically in $v^2/M_{\rm SUSY}^2$. In both matching schemes, we obtain a value for the effective quartic Higgs coupling of the SM, capturing the effects of the heavy particles with masses $\sim M_{\rm SUSY}$ and resumming all large logarithms $\ln(v^2/M_{\rm SUSY}^2)$ consistently via RGEs. Before presenting the calculation of the effective quartic Higgs couplings in the two matching schemes, we show in Fig. 1 our procedure for the computation of the loop-corrected Higgs mass in the EFT approach, implemented in the new version of NMSSMCALC, and describe it in detail in the following.

We start with the six SM input parameters (**box 1a** of Fig. 1) which can be either

$$G_F,\ \alpha_S(M_Z),\ M_t,\ M_W,\ M_Z,\ M_h \tag{3.1}$$

or

$$\alpha(M_Z),\ \alpha_S(M_Z),\ M_t,\ M_W,\ M_Z,\ M_h, \tag{3.2}$$

where all masses are considered to be the pole masses. We call the choice of input parameters of (3.1) the "G_F scheme", while we denote the choice of (3.2) as the "α_{M_Z} scheme". We then have to convert all OS input parameters to their corresponding $\overline{\rm MS}$ parameters at the scale M_t. For the α_{M_Z} scheme we use the conversion formulae which are already available in NMSSMCALC. These conversion formulae have been given in the appendix D of [32], but we use them now at the scale M_t instead of M_Z. For the G_F scheme, we use the conversion formulae at the scale M_t, presented in [57]. Although [57] provides the full two-loop corrections to the conversion formulae, we took into account only one-loop EW corrections for all parameters and two- and three-loop QCD corrections for the conversion of M_t. In addition, we converted between M_h and $\lambda_h^{\rm SM,\overline{MS}}$ at $\mathcal{O}(\alpha_t(\alpha_t+\alpha_s))$. This is the same level of approximation as in the α_{M_Z} scheme.

As running $\overline{\rm MS}$ parameters in the SM, we choose (**box 2**)

$$g_1^{\rm SM,\overline{MS}},\ g_2^{\rm SM,\overline{MS}},\ g_3^{\rm SM,\overline{MS}},\ Y_t^{\rm SM,\overline{MS}},\ v^{\rm SM,\overline{MS}},\ \lambda_h^{\rm SM,\overline{MS}}. \tag{3.3}$$

As usual, we denote by g_1, g_2, g_3 the three gauge couplings of the corresponding three gauge symmetry groups $U(1)_Y$, $SU(2)_L$ and $SU(3)_C$, while Y_t is the top Yukawa coupling. After obtaining these $\overline{\rm MS}$ parameters at M_t, we apply the SM RGEs[4] including full two-loop and partial three- and four-loop contributions [42,58–60] to run up to the matching scale which is denoted by $Q_{\rm match}$ with $Q_{\rm match} \gg M_t$.

For the NMSSM calculation at the high-energy scale $Q_{\rm inp}$ (**box 1b**), we have the following input parameters:

$$v_s,\ \tan\beta,\ m_{\tilde{Q}_3},\ m_{\tilde{u}_{R_3}},\ M_1,\ M_2,\ M_3,\ \lambda,\ \kappa,\ A_t,\ {\rm Re}A_\lambda,\ {\rm Re}A_\kappa,\ \varphi_u,\ \varphi_s \tag{3.4}$$

as well as the corresponding parameters of (3.3) in the $\overline{\rm DR}$ scheme with the exception of the quartic Higgs coupling λ_h, which is not an input parameter in the NMSSM. We remind that the $M_{1,2,3}$ and A_t are complex, their phases are included in the running from $Q_{\rm inp}$ to $Q_{\rm match}$, while the imaginary parts of A_λ and A_κ are eliminated through the tadpole equations at $Q_{\rm match}$. The phases of the other complex parameters, i.e. λ and κ, do not run since their UV-counterterms vanish [33]. Note, that for the sfermion contributions we only take into account corrections from the stops, i.e. the top-quark Yukawa coupling is the only non-zero Yukawa coupling. The first five parameters in **box 1b**), $g_i^{\rm NMSSM,\overline{DR}}$, $Y_t^{\rm NMSSM,\overline{DR}}$ and $v^{\rm NMSSM,\overline{DR}}$, are not fixed as (user) input parameters but actually depend on the values of the running SM-parameters in **box 3**). To solve this two-scale problem, the full set of running SUSY parameters is determined by an iterative RGE running between $Q_{\rm inp}$ and $Q_{\rm match}$ with $X^{\rm NMSSM,\overline{DR}}(Q_{\rm inp}) = X^{\rm SM,\overline{DR}}(Q_{\rm match})$ $(X = g_i, Y_t, v)$ as a first guess, which is symbolised by the double-arrow in

[3] Note that we explicitly distinguish between λ, which is the NMSSM superpotential parameter, and the quartic Higgs coupling in the SM, $\lambda_h^{\rm SM}$.

[4] We employ for g_1 the GUT normalisation $g_1^{\rm GUT} = \sqrt{5/3}g_1$ commonly used in SM RGEs.

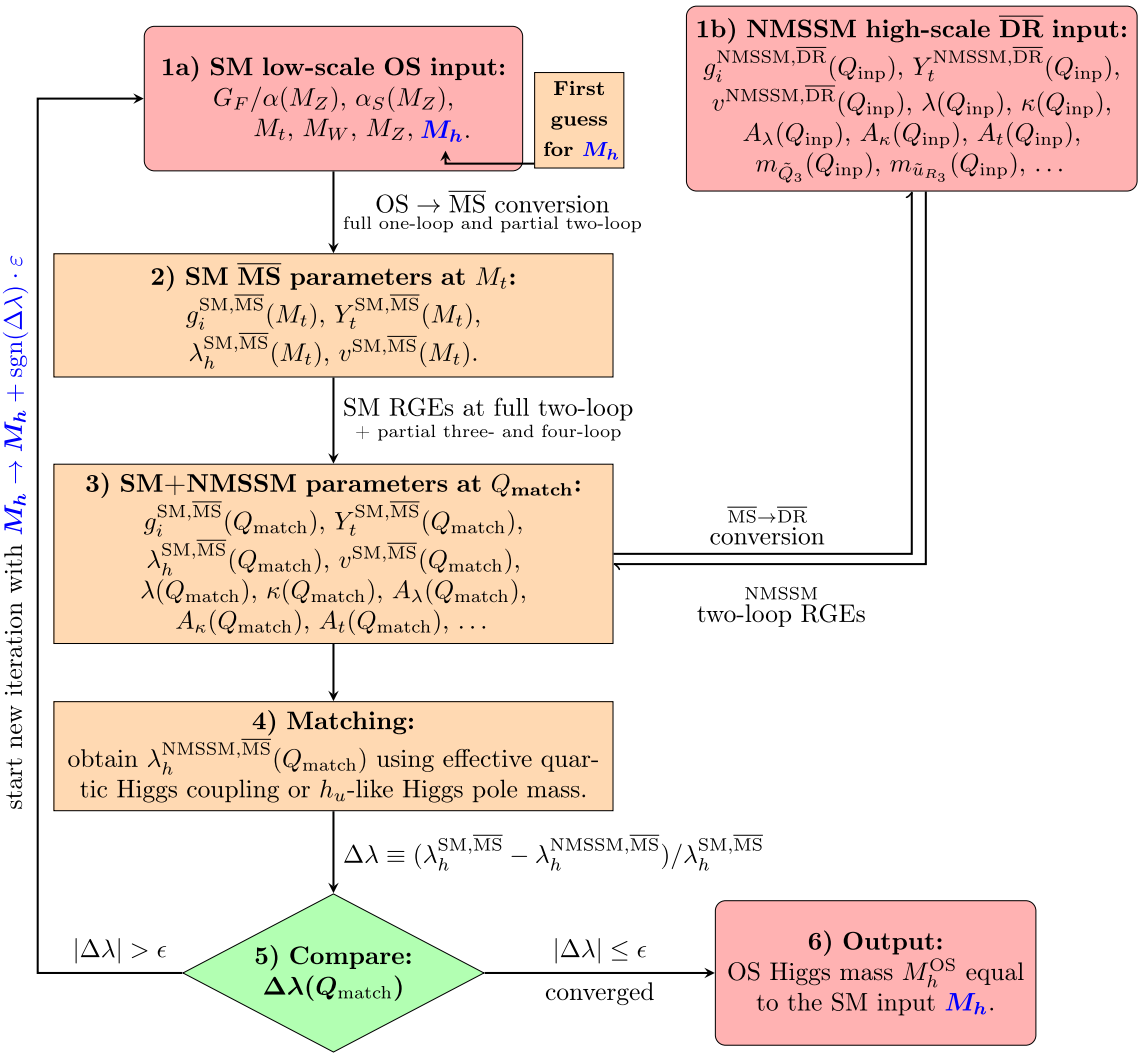

Fig. 1 Schematic procedure for the computation of the loop-corrected Higgs mass in the EFT approach implemented in NMSSMCALC

Fig. 1. The $\overline{\text{MS}} \to \overline{\text{DR}}$ conversion formulae for g_1, g_2 and g_3 between high-scale and low-scale parameters at 1-loop level are given by

$$g_i^{\text{NMSSM},\overline{\text{DR}}} = g_i^{\text{SM},\overline{\text{MS}}} + \delta g_i^{\text{reg}} + \delta g_i^{\text{thr}}, \tag{3.5}$$

where the δg_i^{reg} denote $\overline{\text{MS}}$–$\overline{\text{DR}}$ shifts related to the difference in the regularization schemes [61],

$$\delta g_1^{\text{reg}} = 0, \qquad \delta g_2^{\text{reg}} = \frac{g_2^3}{48\pi^2}, \qquad \delta g_3^{\text{reg}} = \frac{g_3^3}{32\pi^2}, \tag{3.6}$$

and the δg_i^{thr} are the threshold corrections[5] for $v \to 0$ including the effects of the heavy particles which are integrated out in the EFT [55]. They read

$$\delta g_1^{\text{thr}} = -\frac{g_1^3}{512\pi^2}\left[12\ln\frac{|\mu_{\text{eff}}^2|}{Q^2} + 3\ln\frac{m_{H^\pm}^2}{Q^2} + \sum_{i=3}\left(3\ln\frac{m_{\tilde{L}_i}^2}{Q^2} + 6\ln\frac{m_{\tilde{e}_{R,i}}^2}{Q^2}\right) + \sum_{i=1}^{3}\left(\ln\frac{m_{\tilde{Q}_i}^2}{Q^2} + 8\ln\frac{m_{\tilde{u}_{R,i}}^2}{Q^2} + 2\ln\frac{m_{\tilde{d}_{R,i}}^2}{Q^2}\right)\right], \tag{3.7}$$

$$\delta g_2^{\text{thr}} = -\frac{g_2^3}{192\pi^2}\left[8\ln\frac{M_2^2}{Q^2} + 4\ln\frac{|\mu_{\text{eff}}^2|}{Q^2} + \ln\frac{m_{H^\pm}^2}{Q^2} + \sum_{i=3}\left(\ln\frac{m_{\tilde{L}_i}^2}{Q^2} + 3\ln\frac{m_{\tilde{Q}_i}^2}{Q^2}\right)\right], \tag{3.8}$$

[5] The threshold corrections for the gauge couplings can e.g. be obtained from matching the Z and $W^\pm$ boson pole masses as well as the running electromagnetic and strong couplings [50,62].

$$\delta g_3^{\rm thr} = -\frac{g_3^3}{192\pi^2}\left[12\ln\frac{M_3^2}{Q^2} + \sum_{i=1}^{3}\left(2\ln\frac{m^2_{\tilde{Q}_i}}{Q^2} + \ln\frac{m^2_{\tilde{u}_{R,i}}}{Q^2} + \ln\frac{m^2_{\tilde{d}_{R,i}}}{Q^2}\right)\right], \quad (3.9)$$

where $Q = Q_{\rm match}$, and we introduced the effective μ parameter,

$$\mu_{\rm eff} = \lambda\frac{v_s}{\sqrt{2}}e^{i\varphi_s}, \quad (3.10)$$

and $m^2_{H^\pm}$ is given in (2.6). For the top Yukawa coupling, we only require the matching relation at tree level for a consistent calculation of the effective quartic Higgs coupling at 1-loop order,

$$Y_t^{\rm NMSSM,\overline{DR}} = Y_t^{\rm SM,\overline{MS}}/\sin\beta. \quad (3.11)$$

The matching of the VEV will be discussed in Sect. 3.2, as it is not needed for the quartic coupling matching in the unbroken phase, but for the pole mass matching. With the NMSSM $\overline{\rm DR}$ parameters $g_i^{\rm NMSSM,\overline{DR}}$, $Y_i^{\rm NMSSM,\overline{DR}}$, expressed through their low-scale $\overline{\rm MS}$ counterparts, and the other SUSY input parameters of (3.4) at the scale $Q_{\rm match} \sim M_{\rm SUSY}$ (**box 3**), we can then compute the loop corrections in the NMSSM to the quartic Higgs coupling $\lambda_h^{\rm NMSSM,\overline{MS}}(Q_{\rm match})$ of the h_u-like Higgs boson,[6] or to the pole mass of the h_u-like Higgs boson, subtracting the SM corrections consistently and keeping only the pure NMSSM contributions (**box 4**).

Note that in our implementation, we allow the matching scale $Q_{\rm match}$ to be different from the input scale $Q_{\rm inp}$ at which the SUSY parameters of (3.4) are given. In the case of $Q_{\rm match} \neq Q_{\rm inp}$, we use the two-loop NMSSM RGEs as calculated by SARAH [41–44,63–67] to run the SUSY parameters from $Q_{\rm inp}$ to $Q_{\rm match}$. As the Yukawa and gauge couplings are given at $Q_{\rm match}$ (and not $Q_{\rm inp}$) via their low-scale inputs, we thus have to implement the running of the SUSY parameters via an iterative procedure until all parameters converge at the matching scale. We note that due to the RGE running, a CP-violating phase of one of the soft-SUSY-breaking parameters typically induces CP-violating phases also for the other SUSY parameters, so that the CP-violating effects cannot be limited to only one sector of the model.

The obtained loop-corrected $\lambda_h^{\rm NMSSM,\overline{MS}}(Q_{\rm match})$ is then compared to the quartic Higgs coupling of the SM $\lambda_h^{\rm SM,\overline{MS}}(Q_{\rm match})$ of (3.3) at the scale $Q_{\rm match}$ (**box 5**). If the absolute value of the relative difference between the two quartic couplings, $\Delta\lambda \equiv (\lambda^{\rm SM,\overline{MS}} - \lambda^{\rm NMSSM,\overline{MS}})/\lambda^{\rm SM,\overline{MS}}$, is larger than $\epsilon = 10^{-5}$, we change the SM input M_h and, starting again from the top of Fig. 1, iterate the procedure until the precision goal $|\Delta\lambda| < \epsilon$ is reached.[7] In order to efficiently scan over different values of M_h, we use the bisection method for which the procedure converges in logarithmic time. The found value of M_h for which the SM and NMSSM quartic Higgs couplings have the same value at the matching scale $Q_{\rm match}$ (within the precision goal) and at the considered loop order is then identified with our predicted loop-corrected SM-like on-shell Higgs mass in the EFT approach (**box 6**).

To compare the two approaches for the matching conditions, in the numerical discussion in Sect. 4, we will denote the obtained values for the SM-like on-shell Higgs mass by $M_h^{\rm IV}$ for the quartic-coupling matching and by $M_h^{\rm II}$ for the pole-mass matching, i.e. the Roman superscript specifies which scalar n-point function was used in the matching.

3.1 Quartic-coupling matching conditions

We present here our computation of the effective quartic Higgs coupling at the tree and one-loop level after subtracting the SM contributions, i.e. the contributions from all particles which appear in the SM EFT Lagrangian. To improve our prediction, we have included two-loop QCD and mixed QCD-EW corrections as well as the $\mathcal{O}(\alpha_t^2)$ corrections in the limit of the CP-conserving MSSM which are available in SUSYHD [68] and Ref. [69], respectively.[8] Our $\lambda_h^{\rm NMSSM,\overline{MS}}(Q_{\rm match})$ can then be written as the sum of the tree-level, one-loop, and MSSM two-loop parts,

$$\lambda_h^{\rm NMSSM,\overline{MS}}(Q_{\rm match}) = \lambda_h^{\rm NMSSM,tree} + \Delta\lambda_h^{\rm NMSSM,1l} + \Delta\lambda_h^{\rm MSSM,2l}. \quad (3.12)$$

Note, that $\Delta\lambda_h^{\rm MSSM,2l}$ is not sensitive to the CP-violating phases entering $\lambda_h^{\rm NMSSM,tree}$ and $\Delta\lambda_h^{\rm NMSSM,1l}$.

3.1.1 Tree level

At the tree-level the four-h vertex receives contributions from the Feynman diagrams sketched in Fig. 2. Taking into account

[6] By writing $\lambda_h^{\rm NMSSM,\overline{MS}}$, we mean that, while the SUSY calculation is performed in the $\overline{\rm DR}$ scheme, we express the Yukawa and gauge parameters via the low-scale $\overline{\rm MS}$ quantities.

[7] Note that our iterative procedure is slightly different from the one used in [51,52] where in the fifth step, the authors have set $\lambda_h^{\rm SM,\overline{MS}}(Q_{\rm match}) = \lambda_h^{\rm NMSSM,\overline{MS}}(Q_{\rm match})$ and then use the SM RGEs to run $\lambda_h^{\rm SM,\overline{MS}}$ down to the EW scale, where they compare to their input value for the quartic Higgs coupling. Our procedure is, however, quite similar to the one used in [53].

[8] Note that the MSSM results in [68] assume a normalisation of the quartic interaction term in the SM Lagrangian of $-\frac{\lambda_h^{\rm SM}}{2}|H|^4$, so that we have to multiply all MSSM terms by a factor of $\frac{1}{2}$ for our choice of normalisation.

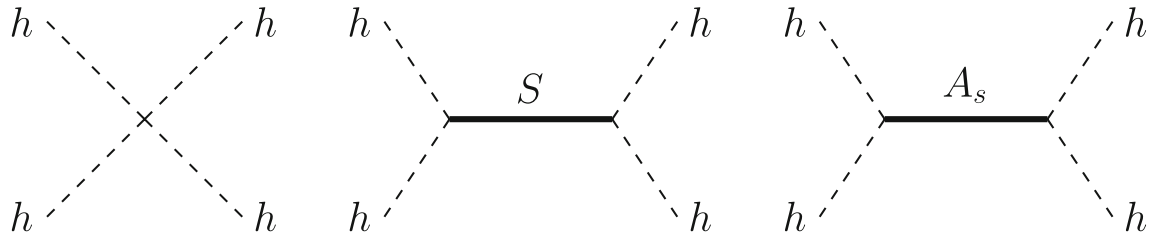

Fig. 2 Exemplary tree-level diagrams which contribute to the tree-level quartic-coupling matching. Thick (thin) lines denote heavy (light) particles which are (not) integrated out in the EFT. The dashed external lines correspond to the SM-like Higgs eigenstate h. The second and third diagrams exhibiting a heavy CP-even (S) or CP-odd (A_s) singlet in the propagator have to be taken into account also for t- and u-channel propagators. Note that the third diagram with the A_s exchange is absent in the CP-conserving case

all tree-level contributions to the effective quartic Higgs coupling, we get the following expression,

$$\lambda_h^{\text{NMSSM,tree}} = \underbrace{\frac{1}{8}(g_1^2+g_2^2)\cos^2 2\beta}_{\text{MSSM } D\text{-terms}} + \underbrace{\frac{1}{4}|\lambda|^2 \sin^2 2\beta}_{\text{NMSSM } F\text{-terms}} \tag{3.13a}$$

$$\underbrace{-\frac{1}{48|\kappa|^2 m_{H_s}^2 (3m_{H_s}^2+m_{A_s}^2)}\Big(3|\kappa|^2 m_{H^\pm}^2 (1-\cos 4\beta) + (3m_{H_s}^2+m_{A_s}^2)\left(|\kappa||\lambda|\cos\varphi_y \sin 2\beta - 2|\lambda|^2\right)\Big)^2}_{s/t/u-\text{ channel } S} \tag{3.13b}$$

$$\underbrace{-\frac{3}{16m_{A_s}^2}|\lambda|^2(3m_{H_s}^2+m_{A_s}^2)\sin^2 2\beta \sin^2\varphi_y}_{s/t/u-\text{ channel } A_s}, \tag{3.13c}$$

where the origin of each term is explained by the corresponding text underneath. While the two contributions of (3.13a) directly originate from the scalar potential in the NMSSM, the terms of Eqs. (3.13b) and (3.13c) arise when the heavy CP-even and CP-odd singlets, appearing as intermediate states in the s-, t-, and u-channels, are integrated out. For simplicity of the expressions in Eqs. (3.13b) and (3.13c) we have used the masses $m_{H_s}^2, m_{A_s}^2, m_{H^\pm}^2$ instead of $v_s, \text{Re}A_\kappa$ and $\text{Re}A_\lambda$. Compared to the CP-conserving case presented in [53], there are additional contributions from the CP-odd singlet field A_s, corresponding to the term in (3.13c). This term will vanish if $\sin\varphi_y = 0$, i.e. if there is no CP-violation at tree-level in the Higgs sector.

3.1.2 One loop

At the one-loop level, the matching condition of the quartic Higgs coupling receives corrections from diagrams involving at least one heavy SUSY particle. In Fig. 3 we show example diagrams, where thick lines correspond to heavy SUSY particles and thin lines to light SM fields. We divide the one-loop corrections into the following six pieces,

$$\Delta\lambda_h^{\text{NMSSM,1l}} = \Delta\lambda_\Box + \Delta\lambda_\triangle + \Delta\lambda_{\text{SE}} + \Delta\lambda_{\text{CT}} + \Delta\lambda_{\text{reg}} + \Delta\lambda_{\text{gauge-thr}}. \tag{3.14}$$

The first four terms correspond to the box, vertex correction, self-energy and counterterm contributions, respectively. The last two terms correspond to the shift induced by the different regularization schemes used in the NMSSM and the SM calculations and the contributions from the matching of the gauge couplings. In all above contributions, diagrams with only SM particles (light states) in the internal lines are discarded, since they belong to the SM contributions and would cancel in the matching condition. All diagrams which contain at least one SUSY particles (heavy state) in the internal lines are kept. Since the momenta of the external Higgs bosons are set to be zero, all four-, three- and two-point one-loop integrals can be reduced to vacuum integrals. For the calculation of the diagrams we make use of the mass- and mixing-matrices of the NMSSM in the unbroken phase of the EW symmetry as specified in Sect. 2.

Box diagrams such as shown in Fig. 3a–d are of similar structure as those which are encountered in the MSSM with the difference that the additional NMSSM degrees-of-freedom are present in the loop. They constitute a separately UV-finite subset. An entirely new type of correction arises in the (complex) NMSSM due to the presence of the non-local contributions at tree-level, *cf.* Fig. 2 second and third diagrams. At the one-loop level, these diagrams receive vertex corrections $\Delta\lambda_\triangle$, propagator corrections $\Delta\lambda_{\text{SE}}$, and corresponding counterterm corrections $\Delta\lambda_{\text{CT}}$ shown exemplary in Fig. 3e–h. The vertex corrections originate from the exchanges of a CP-even or a CP-odd singlet which can be written as

$$\Delta\lambda_\triangle = -\frac{g_{hhS}}{m_{H_s}^2}\Delta g_{hhS} - \frac{g_{hhA_s}}{m_{A_s}^2}\Delta g_{hhA_s} \tag{3.15}$$

where Δg_{hhS}, Δg_{hhA_s} are genuine one-loop contributions to the triple Higgs vertices $h-h-S$ and $h-h-A_s$, respectively, and the trilinear couplings g_{hhS}, g_{hhA_s} are given in (3.19a) and (3.19b), respectively. The propagator corrections come from the one-loop self-energy diagrams of the heavy CP-even

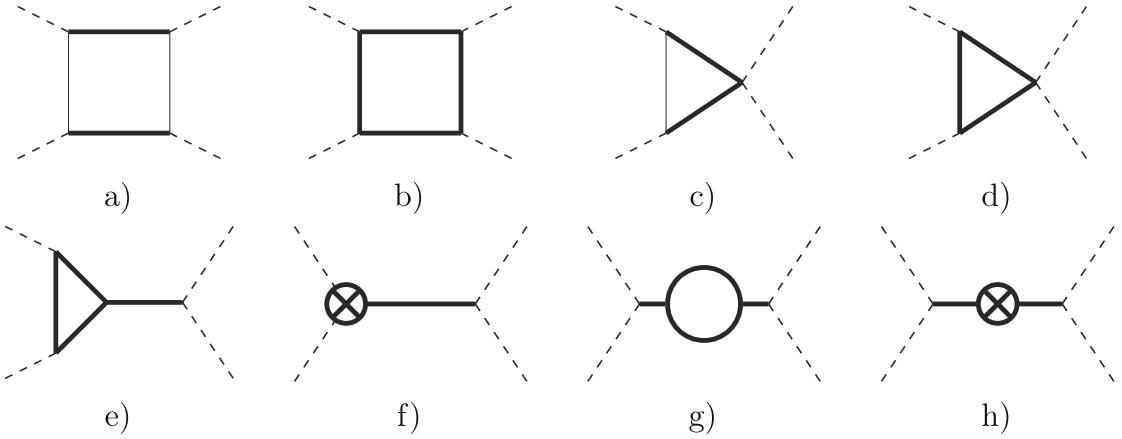

Fig. 3 Selection of one-loop diagrams contributing to the one-loop quartic-coupling matching. Thick (thin) lines denote heavy (light) particles which are (not) integrated out in the EFT. The diagrams **a**–**e**, **g** Show exemplary box, vertex correction and self-energy diagrams, while the diagrams **f**, **h** represent the vertex and mass counterterm diagrams, which implicitly contain contributions from tadpoles

and CP-odd singlet states. They can be expressed as

$$\Delta\lambda_{\rm SE} = -\frac{1}{2}\left(\frac{g_{hhS}}{m^2_{H_s}}\right)^2 \Sigma_{SS}(0) - \frac{1}{2}\left(\frac{g_{hhA_s}}{m^2_{A_s}}\right)^2 \Sigma_{A_sA_s}(0) - \frac{g_{hhA_s} g_{hhS}}{m^2_{A_s} m^2_{H_s}} \Sigma_{SA_s}(0) \tag{3.16}$$

where $\Sigma_{xy}(0)$ $(x, y = S, A_s)$ are the self-energies of the transitions $x \to y$ evaluated at zero external momentum in the limit $v \to 0$. For the counterterm contributions, we note that all parameters appearing explicitly in the tree-level expression in (3.13a) to (3.13c) are renormalised in the $\overline{\rm DR}$ scheme. For the tadpoles, we instead use OS-like renormalisation conditions, such that the minimum of the scalar tree-level potential is identical to the loop-corrected one. At the same time, this choice removes all heavy-light mixing contributions on the external legs of Fig. 2. In the case of the h-H mixing, this is equivalent to working directly in the unbroken phase and using an OS-like counterterm for $\tan\beta$ for the removal of the heavy-light mixing (*cf.* [55]). In the CP-violating case, one also has to deal with h-A mixing which is removed via an OS-like condition for the t_{a_d} tadpole. As a consequence, the counterterm of $\lambda_h^{\rm NMSSM}$ gets UV-finite contributions only from the diagonal wave-function renormalisation constant of the external Higgs fields, the singlet tadpoles and the tadpole of the field a_d. The latter enters via the counterterm of $\mathrm{Im}(A_\lambda)$. We can express $\Delta\lambda_{\rm CT}$ as

$$\Delta\lambda_{\rm CT} = 2\lambda_h^{\rm NMSSM,tree}\delta^{(1)}Z_h - \frac{\delta^{(1)}t_{h_s}}{2v_s}\left(\frac{g^2_{hhS}}{m^4_{H_s}} + \frac{g^2_{hhA_s}}{m^4_{A_s}}\right) + \frac{\delta^{(1)}t_{a_s}}{2v_s}\left(3\frac{g^2_{hhA_s}}{m^4_{A_s}}\tan\varphi_w - 4\frac{g_{hhA_s}g_{hhS}}{m^2_{A_s}m^2_{H_s}} - \frac{g^2_{hhS}}{m^4_{H_s}}\tan\varphi_w\right) + \delta^{(1)}\mathrm{Im}(A_\lambda)\left(\frac{g_{hhA_s}}{m^2_{A_s}}\frac{\partial g_{hhA_s}}{\partial \mathrm{Im}(A_\lambda)} + \frac{g_{hhS}}{m^2_{H_s}}\frac{\partial g_{hhS}}{\partial \mathrm{Im}(A_\lambda)}\right)\Bigg|_{\rm min} \tag{3.17}$$

where the tadpole counterterms $\delta^{(1)}t_{h_s,a_s}$ originate from mass-counterterm inserted diagrams, Fig. 3h, and $\delta^{(1)}\mathrm{Im}A_\lambda$ from the vertex-counterterm inserted diagrams in Fig. 3f. The subscript 'min' indicates that the expression is evaluated at the minimum of the potential (where $\mathrm{Im}(A_\lambda)$ is no input anymore), i.e. using the solutions for the tadpole equations. The Higgs field wave-function renormalisation constant at one-loop order is given by

$$\delta^{(1)}Z_h = -\frac{d\Sigma_{hh}}{dp^2}\bigg|_{p^2=0} \tag{3.18}$$

and the trilinear Higgs couplings related to the singlet states as well as their partial derivatives w.r.t. to $\mathrm{Im}(A_\lambda)$ are

$$g_{hhS} = \frac{1}{2v_s}\left(|\kappa||\lambda|v_s^2\sin(2\beta)\cos\varphi_y - 2|\lambda|^2v_s^2 + m^2_{H^\pm}\sin^2(2\beta)\right), \tag{3.19a}$$

$$g_{hhA_S} = -\frac{3}{2}|\kappa||\lambda|v_s\sin(2\beta)\sin\varphi_y, \tag{3.19b}$$

$$\frac{\partial g_{hhS}}{\partial \mathrm{Im}(A_\lambda)} = -\frac{|\lambda|}{\sqrt{2}}\sin(2\beta)\sin(\varphi_w - \varphi_y), \tag{3.19c}$$

$$\frac{\partial g_{hhA_S}}{\partial \mathrm{Im}(A_\lambda)} = -\frac{|\lambda|}{\sqrt{2}}\sin(2\beta)\cos(\varphi_w - \varphi_y). \tag{3.19d}$$

All other counterterm diagrams are of $\mathcal{O}(v^2/M^2_{\rm SUSY})$ or higher and neglected in the quartic coupling matching. Note, that the couplings in Eqs. (3.19a)–(3.19d) are given at the minimum of the tree-level potential while the derivatives of the couplings have to be evaluated before using the tadpole solutions. Finally, the counterterm of $\mathrm{Im}(A_\lambda)$ is related to

the counterterm of the a_d-tadpole via the tree-level tadpole solution as

$$\delta^{(1)}\mathrm{Im}(A_\lambda) = \frac{\sqrt{2}}{|\lambda| v_s \cos(\varphi_w - \varphi_y)\sin\beta}\frac{\delta^{(1)} t_{a_d}}{v}. \tag{3.20}$$

The above contributions have been obtained by two independent calculations. One calculation relies on `SARAH` [70] to compute the expression for the effective quartic Higgs self-coupling and the other one uses `FeynArts-3.11` [71,72] and `FeynCalc-9.3` [73–75]. Note that in [53], the authors found that in the old version of `SARAH`, a term related to the singlet tadpole was missing. After implementing generic tadpoles into a private version of `SARAH` and computing the singlet tadpole contributions, the results from the two calculations were found to agree. In addition, we performed a non-trivial check of the scale dependence of $\lambda_h^{\mathrm{NMSSM,tree}} + \delta\lambda_h^{\mathrm{NMSSM,11}}$. We tested that the slope of its scale dependence is the same as the slope of the scale dependence of the SM quartic coupling at one-loop level.

At the beginning of this section, we discussed that the quartic-coupling matching is performed in the limit of the unbroken phase, $v \to 0$. This is also the general strategy employed in [62,70]. However, from Eq. (3.20) we can see, that the actual limit $v \to 0$ has to be taken with care in the CP-violating case and requires the expansion of tadpoles up to $\mathcal{O}(v)$. The explicit expansion of $\delta^{(1)} t_{a_d}/v$ up to $\mathcal{O}((v^2/M^2_{\mathrm{SUSY}})^0)$ is derived in Appendix A. It should be stressed, that this situation was not encountered before in e.g. calculations within the CP-violating MSSM: In the MSSM all diagrams that contain $\delta^{(1)} t_i/v$-terms are suppressed by additional powers of v. Therefore, the crucial difference to the pure CP-conserving case is that, in the CP-violating case, the effects of the h-A mixing cannot be entirely removed from the matching condition via the introduction of a finite counterterm. In the language of Ref. [55] this means, while contributions from the counterterm of $\tan\beta$ exactly cancel the h-H mixing in all diagrams (no $\delta\tan\beta$ is left over), the counterterm contributions from the mixing angle that describes the h-A mixing have a left-over finite effect on the matching condition via vertex counterterms as in Fig. 3f.

Finally, we have to take into account the shift due to the NMSSM calculation being done in the $\overline{\mathrm{DR}}$ scheme and the SM contributions being calculated in the $\overline{\mathrm{MS}}$ scheme,

$$\Delta\lambda_{\mathrm{reg}} = \frac{1}{64\pi^2}\left[\frac{g_2^4}{3}\cos^2 2\beta - \frac{1}{2}\left(g_1^4 + 2g_1^2 g_2^2 + 3g_2^4\right)\right]. \tag{3.21}$$

There are two contributions to this shift: The first term in (3.21) accounts for the $\overline{\mathrm{DR}}$–$\overline{\mathrm{MS}}$ conversion of the gauge couplings given in (3.6), since we express all gauge and Yukawa parameters in the threshold corrections to the quartic coupling in (3.14) by their $\overline{\mathrm{MS}}$ values of the low-energy EFT. An additional contribution arises due to diagrams involving quartic couplings between two Higgs and two gauge bosons [70]. As explained above, we discard all diagrams containing only SM-fields i.e. we implicitly subtract these pieces in the $\overline{\mathrm{DR}}$ scheme. However, the subtraction-term strictly would need to be computed in the $\overline{\mathrm{MS}}$ scheme using dimensional regularization rather than dimensional reduction. The second term of (3.21) remedies this mismatch between the two schemes in the subtracted SM contributions.

In addition to the regularisation-scheme shift to the gauge couplings, we also take into account the one-loop gauge thresholds from the matching of the gauge couplings between the NMSSM and the SM,

$$\begin{aligned}\Delta\lambda_{\text{gauge-thr}} &= \lambda_h^{\mathrm{NMSSM,tree}}(g_i \to g_i + \delta g_i^{\mathrm{thr}}) - \lambda_h^{\mathrm{NMSSM,tree}}(g_i)\\ &= \frac{1}{4}\left(g_1\delta g_1^{\mathrm{thr}} + g_2\delta g_2^{\mathrm{thr}}\right)\cos^2 2\beta + \mathcal{O}((\delta g_i)^2),\end{aligned} \tag{3.22}$$

that arise when integrating out all heavy degrees of freedom of the NMSSM. The $\delta g_i^{\mathrm{thr}}$ are defined in Eqs. (3.7) and (3.8). As the singlet states in the NMSSM do not influence the gauge couplings, the shifts of Eqs. (3.21) and (3.22) are identical to the ones of the MSSM [55].

3.2 Pole-mass matching conditions

The pole-mass matching scheme is defined by the condition that the pole-mass of the SM-like Higgs mass eigenstate in the NMSSM[9] is equal to the SM one,

$$(M_h^{\mathrm{SM}})^2 \stackrel{!}{=} (M_h^{\mathrm{NMSSM}})^2. \tag{3.23}$$

The defining equation for the pole-mass in the SM reads

$$0 = p^2 - (m_h^{\mathrm{SM}})^2 + \mathrm{Re}\hat{\Sigma}_h^{\mathrm{SM}}(p^2 = (M_h^{\mathrm{SM}})^2). \tag{3.24}$$

Here, m_h^{SM} denotes the running $\overline{\mathrm{MS}}$ mass of the SM Higgs boson, i.e. the tree-level mass expressed through $\overline{\mathrm{MS}}$ parameters, and $\hat{\Sigma}_h^{\mathrm{SM}}$ is the renormalised one-loop self-energy calculated at a fixed order in the $\overline{\mathrm{MS}}$ renormalisation scheme. The solution $p^2 = (M_h^{\mathrm{SM}})^2$, which fulfills Eq. (3.24) in general has to be found iteratively. The calculation of the pole mass of the SM-like Higgs boson in the NMSSM on the right-hand side of (3.23) is more complicated due to the appearance of multiple Higgs states and their mixing. In general, the pole masses of the Higgs bosons in the NMSSM are the eigenvalues of the loop-corrected Higgs mass matrix $\mathcal{M}_H$,[10]

$$\left(\mathcal{M}_H\right)_{ij} = (m_{h_i}^{\mathrm{NMSSM}})^2\delta_{ij} - \mathrm{Re}\hat{\Sigma}_{ij}^{\mathrm{NMSSM}}(p^2)$$

[9] We remind that we consider the Higgs state to be SM-like if it is predominantly made up of the h_u component.

[10] Here and above for the SM, we use the same sign convention for the self-energy corrections as in [29–33].

$$\text{for } i,\, j = 1, \ldots, 5, \tag{3.25}$$

where $m_{h_i}^{\text{NMSSM}}$ is the tree-level mass of h_i (expressed through the running $\overline{\text{DR}}$ parameters). In NMSSMCALC, the squared tree-level masses are obtained after factorising the Goldstone boson and then diagonalizing the tree-level mass matrix. The eigenvalues are the squared masses that are ordered by ascending mass values. The $\hat{\Sigma}_{ij}^{\text{NMSSM}}(p^2)$ in (3.25) denote the $\overline{\text{DR}}$-renormalised self-energies of the transitions $h_i \to h_j$ at the momentum squared p^2. Similarly to the SM, we take only the real part of the renormalised self-energy for our following discussions. The ith loop-corrected pole mass, $(M_{h_i}^{\text{NMSSM}})^2$, is then obtained by iteratively diagonalizing the mass matrix $\mathcal{M}_H$ until p^2 approaches $(M_{h_i}^{\text{NMSSM}})^2$. However, both the diagonalisation of the loop-corrected mass matrix and the iterative procedure mix different orders of perturbation theory. This mixing can spoil the cancellation of large logarithms by inducing higher powers of $\ln(v^2/M_{\text{SUSY}}^2)$-terms. Thus, an iterative procedure may induce a large theory uncertainty.

In order to obtain a consistent one-loop expansion which is free of any powers of $\ln(v^2/M_{\text{SUSY}}^2)$, we approximate the loop-corrected SM-like Higgs pole mass: We work in the tree-level mass basis as in (3.25). In the following, we assume that the SM-like Higgs state always corresponds to h_1 with the tree-level mass $m_h^{\text{NMSSM}} \equiv m_{h_1}^{\text{NMSSM}}$,

$$(M_h^{\text{NMSSM}})^2 \equiv \big(\mathcal{M}_H\big)_{11} = (m_h^{\text{NMSSM}})^2 - \text{Re}\hat{\Sigma}_{11}^{\text{NMSSM}}\big(p^2\big), \tag{3.26}$$

i.e. we consider only the diagonal element corresponding to the lightest state.[11] At the one-loop level, it is consistent to ignore all mixing self-energy contributions since the diagonalisation of the loop-corrected mass matrix only involves terms proportional to the product of two or more one-loop self-energies.[12] In order to avoid further mixing of orders in the iteration, we take only the first iteration of the pole-mass equation where the momentum squared is set to be equal to the tree-level mass squared, $(M_h^X)^2 = (m_h^X)^2 - \text{Re}\hat{\Sigma}_h^X(p^2 = (m_h^X)^2)$ for $X = \{\text{SM}, \text{NMSSM}\}$. The matching of the pole-masses in the two theories, Eqs. (3.24) and (3.26), is then performed successively: We first evaluate the matching condition at the tree-level which yields $(m_h^{\text{SM}})^2 = (m_h^{\text{NMSSM}})^2$. Using this in the one-loop matching condition, Eq. (3.23), we find

$$(m_h^{\text{SM}})^2 - \text{Re}\hat{\Sigma}_h^{\text{SM}}\big((m_h^{\text{NMSSM}})^2\big) \stackrel{!}{=} (m_h^{\text{NMSSM}})^2 - \text{Re}\hat{\Sigma}_h^{\text{NMSSM}}\big((m_h^{\text{NMSSM}})^2\big), \tag{3.27}$$

where we write $\hat{\Sigma}_h^{\text{NMSSM}} \equiv \hat{\Sigma}_{11}^{\text{NMSSM}}$ to simplify the notation. For a consistent expansion of the matching condition in v^2/M_{SUSY}^2, the real part of the self-energies can furthermore be expanded around small arguments,

$$\text{Re}\hat{\Sigma}_h^X\big((m_h^{\text{NMSSM}})^2\big) = \hat{\Sigma}_h^X(0) + (m_h^{\text{NMSSM}})^2\,\hat{\Sigma}_h^{X\prime}(0) + \mathcal{O}\big((m_h^{\text{NMSSM}})^4\big). \tag{3.28}$$

Using the expansion of Eq. (3.28) in (3.27), the large logarithms $\ln(M_{\text{SUSY}}/v)$ at the matching scale $Q_{\text{match}} \sim M_{\text{SUSY}}$ are the same on the left- and right-hand sides, and the matching condition as a whole is thus free of these logarithms. We finally note that, contrary to e.g. [51], no explicit tadpole contributions are appearing in (3.27), as we define the minimum of our scalar potential to correspond to the tree-level one at all orders ("on-shell tadpole scheme"). Thus, the tadpole contributions are taken into account implicitly via the mass-matrix counterterm included in the renormalised self-energies (see e.g. Appendix G of [32], with all counterterms, other than the ones for the tadpoles, set to zero due to the $\overline{\text{MS}}/\overline{\text{DR}}$ scheme used in our calculation).

The tree-level relation between the $\overline{\text{MS}}$ mass m_h^{SM} and the quartic coupling parameter of the SM Lagrangian in the $\overline{\text{MS}}$ scheme reads

$$(m_h^{\text{SM}})^2 = 2(v^{\text{SM}})^2\,\lambda_h^{\text{SM},\text{II}}, \tag{3.29}$$

where v^{SM} is the VEV of the SM in the $\overline{\text{MS}}$ scheme.[13] Using this relation, (3.27) implicitly defines a matching condition for the quartic coupling and therefore allows to extract a prediction for the effective quartic coupling of the SM-like Higgs in the NMSSM at the matching scale, which we will denote for consistency with the above notation as $\lambda_h^{\text{NMSSM},\overline{\text{MS}},\text{II}}$. Contrary to the quartic-coupling matching, the appearance of the VEV in (3.29) prevents us from setting $v \to 0$ right from the beginning. The pole-mass matching thus requires a double expansion in the loop order as well as in v^2/M_{SUSY}^2. Solving (3.27) for the quartic coupling appearing in (3.29), the pole-mass matching condition can then be cast in a similar form as the quartic-coupling matching:

$$\lambda_h^{\text{NMSSM},\overline{\text{MS}},\text{II}} = \lambda_h^{\text{NMSSM},\text{tree},\text{II}} + \Delta\lambda_h^{\text{NMSSM},1\text{l},\text{II}} + \Delta\lambda_h^{\text{MSSM},2\text{l}}, \tag{3.30}$$

where we again improve our result by adding the two-loop MSSM corrections of [68,69] as in the case of the quartic-coupling matching in (3.12). We introduce the additional

[11] For the pole-mass matching implemented in NMSSMCALC the SM-like Higgs is not required to be the lightest Higgs state (h_1), but could also be a heavier state. However, in such scenarios our EFT approach may not be valid any more and the result has to be taken with care.

[12] It can be seen that, when diagonalizing (3.25) and then expanding in the self-energies, the off-diagonal self-energy corrections with $i \neq j$ only contribute at two-loop order or higher.

[13] The v^{SM} is gauge dependent, which, however, we have not investigated in this study. We work in the 't Hooft-Feynman gauge throughout all parts of the calculation. Some discussions and investigations of the gauge dependence can be found in [76,77].

superscript $\mathbb{I}$ in order to distinguish the effective quartic coupling obtained via approach from the corresponding one of the quartic-coupling matching approach in (3.12), since the former includes also partial $v^2/M_{\rm SUSY}^2$ terms.

The pole mass obtained in the NMSSM depends on the VEV as defined in the high-energy theory, $v^{\rm NMSSM}$. As we want to express the matching condition only in terms of either $v^{\rm NMSSM}$ or $v^{\rm SM}$, it is thus also required to match the VEV and take into account the shift between the two,

$$(v^{\rm SM})^2 = (v^{\rm NMSSM})^2 + \delta v^2 = (v^{\rm NMSSM})^2 \left(1 + \frac{\delta v^2}{v^2}\right). \tag{3.31}$$

In the last term of (3.31), we do not distinguish between $v^{\rm SM}$ and $v^{\rm NMSSM}$, as the difference is of higher order. The threshold correction δv^2 can be obtained from matching e.g. the Z-boson pole mass at one loop in the SM and the NMSSM, which can futhermore be related through Ward identities to the wave-function renormalisation of the Higgs boson [62],

$$\frac{\delta v^2}{v^2} = \left[\hat{\Sigma}_h^{\rm NMSSM\prime}(0) - \hat{\Sigma}_h^{\rm SM\prime}(0)\right] + \mathcal{O}(v^2/M_{\rm SUSY}^2), \tag{3.32}$$

where $\hat{\Sigma}_h^{X\prime}$ denotes the first derivative of the self energy with respect to the four-momentum squared.

Analogously to the quartic-coupling matching, we express the gauge and Yukawa couplings entering the NMSSM self-energies in terms of the $\overline{\rm MS}$ quantities of the low-energy effective theory. Thus, we use a tree-level matching of the Yukawa couplings due to their appearance only starting from one loop, and the one-loop matching for the gauge couplings of (3.5). If we were to simply plug (3.5) into the tree-level mass term $(m_h^{\rm NMSSM})^2$ of (3.27), we would induce partial two-loop contributions and higher (possibly spoiling the cancellation of large logarithms). In order to include the gauge shifts consistently at the one-loop order, we expand the tree-level mass in $\delta g_i = \delta g_i^{\rm reg} + \delta g_i^{\rm thr}$ $(i = 1, 2)$ to first order

$$\begin{aligned}\left(m_h^{\rm NMSSM}\right)^2 &\equiv \left(m_h^{\rm NMSSM}(g_i^{\rm NMSSM,\overline{DR}} \to g_i^{\rm SM,\overline{MS}} + \delta g_i)\right)^2 \\ &= \left(m_h^{\rm NMSSM,tree}(g_i^{\rm SM,\overline{MS}})\right)^2 + \delta^{\rm gauge} m_h^2 + \mathcal{O}((\delta g_i)^2)\end{aligned} \tag{3.33}$$

The pole-mass matching involves a rotation into the mass basis,

$$\delta^{\rm gauge} m_h^2 = \left(\mathcal{R}^H(v)\delta^{\rm gauge}\boldsymbol{M}_H\mathcal{R}^{H^T}(v)\right)_{11}, \tag{3.34}$$

where $\mathcal{R}^H(v)$ are the rotation matrices that diagonalise the squared neutral Higgs mass matrix, $\mathcal{R}^H(v)\boldsymbol{M}_H\mathcal{R}^{H^T}(v) = (m_{h_i}^{\rm NMSSM})^2\delta_{ij}$, in the broken phase (i.e. not as in Eq. (2.10) but for the case of non-zero v) and

$$\delta^{\rm gauge}\boldsymbol{M}_H = \sum_{i=1,2}(\delta g_i^{\rm thr} + \delta g_i^{\rm reg})\frac{\partial}{\partial g_i^{\rm NMSSM,\overline{DR}}}\boldsymbol{M}_H\bigg|_{g_i^{\rm NMSSM,\overline{DR}} \to g_i^{\rm SM,\overline{MS}}}. \tag{3.35}$$

With this treatment we guarantee that all logarithms of the form $\ln v/Q_{\rm match}$ appearing in the electroweak corrections can cancel in the pole-mass matching while we still correctly take into account the leading corrections from the $\overline{\rm DR} - \overline{\rm MS}$ conversion. However, in the numerical analysis we found that these effect are numerically small compared to e.g. the stop contributions.

3.2.1 Tree level

Keeping only the lowest-order terms of (3.27) and setting the self-energy corrections to zero, we obtain together with (3.29) the condition

$$(m_h^{\rm SM})^2 = 2(v^{\rm SM})^2\,\lambda_h^{\rm SM,\mathbb{I}} \stackrel{!}{=} (m_h^{\rm NMSSM})^2. \tag{3.36}$$

At lowest order, we do not have to take into account the threshold corrections to the VEV, so we can set $v^{\rm SM} = v^{\rm NMSSM}$ with $\delta v^2 = 0$. Furthermore, the right-hand side of (3.36) is expressed via the SUSY and the low-energy $\overline{\rm MS}$ gauge parameters only, so that we also set $\delta m^2_{h,\rm gauge}$ of (3.34) to zero. Equation (3.36) thus becomes the tree-level matching relation for the effective quartic coupling:

$$\lambda_h^{\rm SM,\mathbb{I}} \stackrel{!}{=} \frac{(m_h^{\rm NMSSM})^2}{2(v^{\rm NMSSM})^2} \equiv \lambda_h^{\rm NMSSM,tree,\mathbb{I}}. \tag{3.37}$$

We have checked that, by analytically diagonalizing the tree-level Higgs mass matrix in the NMSSM with full VEV dependence to obtain $m_h^{\rm NMSSM}$ and then expanding (3.37) in $v^2/M_{\rm SUSY}^2$, the same expression as in Eqs. (3.13a)–(3.13c) is obtained at the lowest order $\mathcal{O}((v^2/M_{\rm SUSY}^2)^0)$.

3.2.2 One loop

At one-loop order, we take into account the one-loop self energies in (3.27), and obtain after plugging in (3.29):

$$\begin{aligned}&2(v^{\rm SM})^2\,\lambda_h^{\rm SM,\mathbb{I}} - \hat{\Sigma}_h^{\rm SM}\left((m_h^{\rm NMSSM})^2\right) \stackrel{!}{=} (m_h^{\rm NMSSM})^2 \\ &\quad - \hat{\Sigma}_h^{\rm NMSSM}\left((m_h^{\rm NMSSM})^2\right),\end{aligned} \tag{3.38}$$

which results in the expression for the effective quartic coupling:

$$\begin{aligned}\lambda_h^{\mathrm{SM},\mathrm{II}} &\stackrel{!}{=} \frac{1}{2(v^{\mathrm{SM}})^2}\Big[(m_h^{\mathrm{NMSSM}})^2 - \hat{\Sigma}_h^{\mathrm{NMSSM}}\big((m_h^{\mathrm{NMSSM}})^2\big) \\ &\quad + \hat{\Sigma}_h^{\mathrm{SM}}\big((m_h^{\mathrm{NMSSM}})^2\big)\Big] \\ &\equiv \lambda_h^{\mathrm{NMSSM,tree,II}} + \Delta\lambda_h^{\mathrm{NMSSM,1l,II}}.\end{aligned} \tag{3.39}$$

To extract the leading terms in the expansion of v^2/M_{SUSY}^2, we replace v^{SM} by v^{NMSSM} according to Eqs. (3.31) and (3.32), and we expand the self-energies according to (3.28), so that eventually, we obtain for the one-loop contribution to the matching condition:

$$\Delta\lambda_h^{\mathrm{NMSSM,1l,II}} = -\frac{1}{2(v^{\mathrm{NMSSM}})^2}\Big[\Delta\hat{\Sigma}_h + 2(m_h^{\mathrm{NMSSM}})^2\Delta\hat{\Sigma}_h'\Big], \tag{3.40}$$

where we have introduced the abbreviation $\Delta\hat{\Sigma}_h^{(\prime)} \equiv \hat{\Sigma}_h^{\mathrm{NMSSM}(\prime)}(0) - \hat{\Sigma}_h^{\mathrm{SM}(\prime)}(0)$. The last term of (3.40) can for $v \to 0$ immediately be identified with the first term of (3.17), corresponding to the wave-function-renormalisation contribution. In the tree-level piece of (3.39), given via (3.37), we apply the replacement of (3.34) in order to take into account the $\overline{\mathrm{DR}}$-$\overline{\mathrm{MS}}$ and gauge threshold shifts consistently at the one-loop order. Then, (3.39) is again expressed through the SUSY input parameters as well as the $\overline{\mathrm{MS}}$ parameters of the low-energy theory only.

The self-energies and wave-function renormalisation contributions required for the calculation of the pole-mass matching at one loop are identical to the ones used for fixed-order calculations of the pole masses, and we can therefore reuse the available expressions in the `NMSSMCALC` code after modifying the counterterms such that the self-energies, which are given in the code in a mixed on-shell–$\overline{\mathrm{DR}}$ scheme, are renormalised purely in the $\overline{\mathrm{DR}}$ scheme.[14]

As the pole-mass matching procedure depends non-trivially on the value of the VEV due to the tree-level mass diagonalisation, and relies on numerical cancellations between different terms, the VEV cannot be set to zero exactly, and the suppressed v^2/M_{SUSY}^2 terms are thus always included.[15] As a cross check of the consistent one-loop implementation of the pole-mass matching procedure, we have numerically evaluated the matching procedure for an artificially small value of $v \sim 1$ GeV to decrease the size of the v^2/M_{SUSY}^2 terms, and found in general very good agreement with the quartic-coupling matching approach of Sect. 3.1, see the discussion in Sect. 4.5.2.

Finally, we also include two-loop MSSM corrections [68, 69] to the matching condition, see (3.30). However, unlike the one-loop results obtained with the pole-mass matching, the two-loop results are not sensitive to v^2/M_{SUSY}^2 terms or CP-violating phases.

3.3 Uncertainty estimate

In this section we describe the method used to estimate different theoretical uncertainties entering the Higgs mass prediction. For a review of commonly considered uncertainties see e.g. Ref. [8]. It is useful to distinguish between two sources of uncertainty which originate in relations used at the low-energy electroweak scale (SM uncertainty) and at the high-energy matching scale (SUSY uncertainty).

SM uncertainties: The uncertainty originating from relations at the low-energy scale contains different components:

- Missing electroweak corrections in the extraction of SM $\overline{\mathrm{MS}}$ parameters are estimated by choosing either the Fermi constant G_F or the fine structure constant α_{M_Z} as an input and adapting the renormalisation of the electroweak sector accordingly using either the G_F-scheme [38] or the α_{M_Z}-scheme [33]. Note that we treat the level a We denote the difference in the Higgs mass prediction between the two renormalisation schemes by

$$\Delta_{G_F/\alpha_{M_Z}}^{\mathrm{SM}} = \left|M_h^{G_F} - M_h^{\alpha_{M_Z}}\right|. \tag{3.41}$$

- To estimate missing higher-order corrections in the relation between $\lambda^{\mathrm{SM},\overline{\mathrm{MS}}}$ and the Higgs pole-mass beyond the gauge-less limit, we take the $\overline{\mathrm{MS}}$ parameters (obtained in step 2 of Fig. 1), run them to $Q_{\mathrm{EW}} = M_t/2$ and $2M_t$, respectively, using SM RGEs and compute the Higgs pole-mass at the two-loop order in the $\overline{\mathrm{MS}}$ scheme by solving

$$\begin{aligned}0 = {} & p^2 - 2\lambda_h^{\mathrm{SM},\overline{\mathrm{MS}}}(Q_{\mathrm{EW}})v^2(Q_{\mathrm{EW}}) \\ & + \mathrm{Re}\,\Sigma_h(p^2, Q_{\mathrm{EW}})|_{\mathrm{UV-fin}}\end{aligned} \tag{3.42}$$

iteratively for $p^2 = M_h^{\overline{\mathrm{MS}},\mathrm{pole}}(Q_{\mathrm{EW}})$. In Eq. (3.42) we evaluate the UV-finite part of the Higgs self-energy in the $\overline{\mathrm{MS}}$ scheme at the full one-loop level and take into account the leading two-loop $\mathcal{O}(\alpha_t(\alpha_t + \alpha_s))$ corrections, obtained with `FeynCalc` and `TARCER`. As a reference point we use the OS Higgs pole-mass from step

[14] We note that this procedure thus requires the use of Re A_λ as a $\overline{\mathrm{DR}}$ input parameter instead of the on-shell input for the charged Higgs mass $m_{H^\pm}$

[15] We want to note that we include the dominant v^2/M_{SUSY}^2 terms, neglect, however, some numerically small v^2/M_{SUSY}^2 contributions arising from e.g. the matching of the gauge couplings, which we do for an exactly vanishing VEV $v \to 0$.

1a and estimate the uncertainty as

$$\Delta^{\rm SM}_{Q_{\rm EW}} = \max\left\{\left|M_h^{\rm OS} - M_h^{\overline{\rm MS},{\rm pole}}(2M_t)\right|, \left|M_h^{\rm OS} - M_h^{\overline{\rm MS},{\rm pole}}(M_t/2)\right|\right\}. \tag{3.43}$$

Since these shifts are not symmetric around M_t, we take the maximum of the two differences. The estimate is performed for a fixed electroweak scheme which can be chosen in the SLHA input file (α_{M_Z} or G_F).

- The third component computes the Higgs boson mass while adding/removing three-loop (and higher-order) corrections to the $\overline{\rm MS}$ top quark Yukawa coupling:

$$\Delta^{\rm SM}_{Y_t} = M_h(Y_t^{\mathcal{O}(\alpha_s^2)}) - M_h(Y_t^{\mathcal{O}(\alpha_s^3)}). \tag{3.44}$$

This shift has been obtained numerically using the code mr for $m_h = 125.1\,\text{GeV}$ and $M_t = 172.76\,\text{GeV}$. The three-loop shift is negative and typically causes a decrease of the effective SM Higgs mass of about $\sim 800\,\text{MeV}$.

It should be noted that the three types of uncertainties are not completely independent from each other with the exception of $\Delta^{\rm SM}_{G_F/\alpha_{M_Z}}$ and $\Delta^{\rm SM}_{Y_t}$, which can be considered to be independent.

SUSY uncertainties: For the estimate of the high-scale uncertainty, we generated the two-loop RGEs for the CP-violating NMSSM using SARAH and implemented them in NMSSMCALC. As stated before, the matching scale and the SUSY scale (defining the scale of the SUSY $\overline{\rm DR}$ input parameters) do not need to be the same. We change the matching scale in the range of $[M_{\rm SUSY}/2, 2M_{\rm SUSY}]$, and then compare to the result obtained with $Q_{\rm match} = M_{\rm SUSY}$. It should be noted that these shifts are not symmetric around $Q_{\rm match} = M_{\rm SUSY}$ and therefore we take the maximum of the two differences as

$$\Delta^{\rm SUSY}_{Q_{\rm match}} = \max\{\left|M_h^{M_{\rm SUSY}/2} - M_h^{M_{\rm SUSY}}\right|, \left|M_h^{2M_{\rm SUSY}} - M_h^{M_{\rm SUSY}}\right|\}. \tag{3.45}$$

To estimate the uncertainty of missing higher-order corrections to the matching condition which are not scale-dependent, one typically changes the definition of the top-quark Yukawa coupling entering the matching condition. The structure of the NMSSM-specific component of this type of uncertainty was already discussed in Ref. [53]. Since we plan to include exactly this type of missing higher-order corrections via a pole-mass matching using the results of Ref. [33] in the near future, we also leave the corresponding uncertainty estimate for future work.

Combined uncertainty: The total uncertainty is computed by assuming independent individual uncertainties,

$$\Delta M_h^{\rm II} = \left[\left(\Delta^{\rm SM}_{G_F/\alpha_{M_Z}}\right)^2 + \left(\Delta^{\rm SM}_{Q_{\rm EW}}\right)^2 + \left(\Delta^{\rm SM}_{Y_t}\right)^2 + \left(\Delta^{\rm SUSY}_{Q_{\rm match}}\right)^2\right]^{\frac{1}{2}}. \tag{3.46}$$

As stated above, not all uncertainties are independent of each other. Therefore, the total uncertainty computed by NMSSMCALC is a rather conservative estimate. Equation (3.46) is used to estimate the uncertainty of the Higgs mass prediction if the pole-mass matching was chosen in the SLHA input. If the quartic coupling matching was chosen, the uncertainty is given by

$$\Delta M_h^{\rm IV} = \Big[\left(\Delta M_h^{\rm II}\right)^2 + \underbrace{(M_h^{\rm II} - M_h^{\rm IV})^2}_{\equiv \Delta^{\rm SUSY}_{v^2/M^2_{\rm SUSY}}}\Big]^{\frac{1}{2}}, \tag{3.47}$$

which takes the missing $v^2/M^2_{\rm SUSY}$-terms into account and is labeled as a third uncertainty[16], the *EFT uncertainty* $\Delta^{\rm SUSY}_{v^2/M^2_{\rm SUSY}}$, in Ref. [8].

4 Numerical results

In this section we investigate the results for the SM-like Higgs boson mass prediction numerically using the implementation in NMSSMCALC. We first perform a numerical cross-check of our result by comparing with the findings of Ref. [53]. Furthermore, we investigate the size of the $v^2/M^2_{\rm SUSY}$ corrections in different corners of the parameter space by comparing results obtained with either the pole-mass or quartic-coupling matching and investigate the size of the individual uncertainty components. Finally we also discuss the effects of CP-violating phases on the Higgs mass prediction.

4.1 Setup and applied constraints

The physical SM input parameters used in step 1a of Fig. 1 are

$$\begin{aligned} G_F &= 1.1663788\times10^{-5}\ \text{GeV}^{-2}, & \alpha(M_Z) &= 1/127.955,\\ \alpha_s(M_Z) &= 0.1181, & M_t &= 172.69\ \text{GeV},\\ m_b^{\overline{\rm MS}} &= 4.18\ \text{GeV}, & M_\tau &= 1.77682\ \text{GeV},\\ M_W &= 80.377\ \text{GeV}, & M_Z &= 91.1876\ \text{GeV}, \end{aligned} \tag{4.1}$$

[16] Note that, $M_h^{\rm II}$, $M_h^{\rm IV}$ are both computed at the same order of approximation. In an abuse of language we call the difference between them "uncertainty" to address the missing $v^2/M^2_{\rm SUSY}$ effect of the quartic coupling matching result.

where either G_F or α_{M_Z} is used as an input depending on the renormalisation scheme choice, *cf.* Sect. 3.[17]

In order to investigate the difference between the two matching procedures and the FO calculation (in the $\overline{\text{DR}}$ scheme) and to assess the reliability of each calculation in different corners of the NMSSM parameter space, we have performed a parameter scan varying the NMSSM input parameters uniformly in the following ranges,

$$\begin{aligned} 100\,\text{GeV} \leq M_1, M_2 \leq 1.5\,\text{TeV}, \quad & 100\,\text{GeV} \leq \mu_{\text{eff}} \leq 1.5\,\text{TeV}, \\ 1\,\text{TeV} \leq m_{\tilde{Q}_{L_3}}, m_{\tilde{t}_{R_3}} \leq 2.5\,\text{TeV}, \quad & M_{\text{SUSY}} = \sqrt{m_{\tilde{Q}_{L_3}} m_{\tilde{t}_{R_3}}}, \\ M_3 = \max\{M_{\text{SUSY}}, 2.3\,\text{TeV}\}, \quad & -2.5\,\text{TeV} \leq A_\kappa \leq 100\,\text{GeV}, \\ -2.5\,\text{TeV} \leq A_\lambda \leq 2.5\,\text{TeV}, \quad & -\sqrt{6} \leq \hat{X}_t \leq \sqrt{6}, \\ 1 \leq \tan\beta \leq 20, \quad & 0.05 \leq \lambda, \kappa \leq 1.0\,. \end{aligned} \tag{4.2}$$

All soft-SUSY-breaking trilinear couplings are set equal to $A_i = \hat{X}_t M_{\text{SUSY}} + \mu_{\text{eff}}/\tan\beta$, whereas all left- and right-handed soft-SUSY-breaking sfermion masses are set equal to $m_{\tilde{Q}_{L_3}}$ and $m_{\tilde{t}_{R_3}}$, respectively. The input scale is set to $Q_{\text{inp}} = M_{\text{SUSY}}$. In order to simplify the scan we set all CP-violating phases to zero and instead study the influence of CP-violation for individual parameter points in Sect. 4.5. Note that within this scan, we do not restrict the masses of the SUSY particles to be very heavy such that parameter regions suitable for a fixed-order as well as for the EFT calculation (and intermediate regions) are contained in the sample. However, we put a lower bound on the masses of SUSY particles according to the null search results at LEP and LHC [78] as follows:

$$\begin{aligned} M_{\chi^0,\chi^\pm} > 200\,\text{GeV}, \quad M_{\tilde{t}_1} > 1310\,\text{GeV}, \\ M_{\tilde{g}} > 2300\,\text{GeV}, \quad M_{H^+} > 500\,\text{GeV}. \end{aligned} \tag{4.3}$$

The constraints on all other sfermion masses are automatically fulfilled since the sfermions are approximately mass-degenerate in the chosen parametrisation. We demand that the lightest neutral CP-even Higgs boson is the SM-like Higgs boson (by requiring an h_u component of at least 50%). Its mass is required to lie in the range

$$122\,\text{GeV} \leq M_h^{\text{II}} \leq 128\,\text{GeV}. \tag{4.4}$$

It should be noted that scenarios where the SM-like Higgs boson is not the lightest scalar state are not excluded by current measurements. However, in these scenarios the SM is not the right EFT (rather a singlet-extended SM needs to be considered) and therefore we exclude them from the scan. We use `HiggsTools` [79], which contains `HiggsBounds` [80], to check if the parameter points pass all the exclusion limits from the searches at LEP, Tevatron and the LHC, and `HiggsSignals` [81] to check if the points are consistent with the LHC data for a 125 GeV Higgs boson within 2σ. We do so by requiring $\Delta\chi^2 = \left|\chi^2_{M_{\text{SUSY}}\to\infty} - \chi^2_i\right| < 6.18$, where χ^2_i is the χ^2-value computed by `HiggsSignals` (assuming a fix mass-uncertainty of ± 3 GeV for all Higgs boson masses) for the specific parameter point and $\chi^2_{M_{\text{SUSY}}\to\infty}$ is a SM-reference point obtained in the decoupling limit.[18] We furthermore require that $\lambda^2 + \kappa^2 \leq 1$, which slightly relaxes the requirement of perturbative unitarity below the GUT-scale [82].

Concerning the concrete setup in `NMSSMCALC` we chose to apply the constraints on the spectrum computed with the pole-mass matching since this method promises to give precise results for both low and high SUSY masses. In addition, `NMSSMCALC` computes and provides individual results for M_h using the quartic-coupling matching and the old fixed-order calculation, *cf.* Appendix B.

In the following we also discuss three individual parameter points `BP{1,2,3}`. We list their input parameters in Table 1 and a subset of the resulting mass spectra in Tables 2 and 3. The benchmark points `BP1` and `BP2` are taken from Refs. [53] and [8] and have a BSM mass spectrum which is at or above 2.5 TeV. The parameter point `BP3` is part of the scan sample described above and features a rather light singlet-light state, $M_{h_2} \approx 300$ GeV, which mixes to approximately 4% with the SM-like Higgs boson. `BP1` and `BP3` feature relatively large λ and κ while `BP2` is given in the MSSM-limit. This choice of parameters enables us to compare with the literature as well as to study NMSSM-specific scenarios in the EFT-context not considered before.

4.2 Uncertainties

In Table 4 we list the individual uncertainties contributing to the total uncertainty as defined in Sect. 3.3 for the benchmark points `BP{1,2,3}`. The two dominant sources are the SUSY scale-uncertainty and missing higher-orders in the extraction of the SM top-quark coupling followed by the SM scale-uncertainty which are all between about 200–800 MeV (in absolute values). The SUSY scale-uncertainty is particularly large for the point `BP3` which is due to its BSM mass spectrum being spread across both the electroweak and the TeV-scale. The uncertainty due to the scheme choice between α_{M_Z} and G_F, $\Delta^{\text{SM}}_{G_F/\alpha_{M_Z}}$, is always smaller than 100 MeV indicating that the missing two-loop electroweak corrections in the SM-part of `NMSSMCALC` are rather small.

If the quartic-coupling matching is considered, the missing v^2/M^2_{SUSY} corrections, $\Delta^{\text{SUSY}}_{v^2/M^2_{\text{SUSY}}}$, also contribute to the total uncertainty ΔM_h^{IV}. These corrections are particularly

[17] The bottom and τ masses are needed in the fixed-order calculations.

[18] With the current `HiggsSignals` dataset we find $\chi^2_{M_{\text{SUSY}}\to\infty} \approx 152.1$, which is reasonably close to $\chi^2 \approx 152.5$ found with the built-in reference model `SMHiggsEW` of `HiggsTools`.

Table 1 The most relevant input parameters for the Higgs boson mass prediction chosen for three benchmark points considered in this work (rounded to two digits). All parameters with mass dimension one are given in units of TeV. BP3 is part of the scan sample obtained in this work, BP1 was taken from Ref. [53], Fig. 2 and BP2 from Ref. [8], Fig. 5. The complete set of input parameters can be found on the webpage of the program

	$\tan\beta$	λ	κ	M_1	M_2	M_3	A_t	A_λ	A_κ	μ_{eff}	$m_{\tilde{Q}_{L_3}}$	$m_{\tilde{t}_{R_3}}$	References
BP1	3.0	0.6	0.6	1.0	2.0	2.5	12.75	0.3	− 2.0	1.5	5.0	5.0	[53]
BP2	20.0	0.05	0.05	4.5	4.5	4.5	− 10.79	− 4.28	− 1.5	4.5	4.5	4.5	[8]
BP3	1.27	0.73	0.62	0.24	1.18	2.3	− 0.39	0.06	− 1.44	0.49	1.79	1.51	This work

Table 2 Neutral and charged Higgs boson masses derived from the input parameters in Table 1 using NMSSMCALC. All values are given in units of GeV. For neutral CP-even/odd Higgs bosons we indicate the dominant gauge-eigenstate admixture in brackets. The lightest neutral Higgs boson was computed using the pole-mass (M_h^{II}) and quartic-coupling (M_h^{IV}) matching approaches. All other BSM Higgs boson masses are computed in the $\overline{\text{DR}}$ scheme with the highest-available but fixed order in NMSSMCALC

	M_h^{II}	M_h^{IV}	M_{h_2}	M_{h_3}	M_{A_1}	M_{A_2}	M_{H^+}
BP1	124.29 (h_u)	124.31 (h_u)	2407.6 (h_s)	2971.8 (h_d)	2905.7 (a)	3000.2 (a_s)	2967.1
BP2	125.15 (h_u)	125.15 (h_u)	4486.6 (h_d)	8616.7 (h_s)	4510.9 (a_s)	4984.0 (a)	4995.0
BP3	127.16 (h_u)	129.46 (h_u)	305.5 (h_s)	659.5 (h_d)	663.8 (a)	1308.7 (a_s)	658.4

Table 3 Excerpt of the SUSY mass spectrum derived from the input parameters in Table 1 using NMSSMCALC. All values are given in units of GeV

	$m_{\tilde{t}_1}$	$m_{\tilde{t}_2}$	$m_{\chi_1^0}$	$m_{\chi_2^0}$	$m_{\chi_3^0}$	$m_{\chi_4^0}$	$m_{\chi_5^0}$	$m_{\chi_1^+}$	$m_{\chi_2^+}$
BP1	4829.6	5168.2	997.2	1491.5	1502.4	2010.5	3003.3	1490.2	2010.5
BP2	4335.2	4662.4	4432.6	4500.0	4500.0	4567.8	9000.0	4407.2	4559.9
BP3	1514.2	1799.1	232.8	484.1	498.2	835.4	1192.7	477.3	1192.6

important for the parameter point BP3 as it features a rather light singlet. We find that the total uncertainty of BP3 is shifted from $\mathcal{O}(900\,\text{MeV})$ to about $\mathcal{O}(2\,\text{GeV})$ when using the quartic-coupling matching instead of the pole-mass matching. The effect of the light singlet and the interplay with the v^2/M_{SUSY}^2 corrections is studied in Sect. 4.4 in more detail.

4.3 Numerical validation and comparison with previous works

In this section we numerically validate the calculation and implementation of the two matching procedures in NMSSMCALC. The one-loop matching condition for the quartic coupling has previously been computed in e.g. Ref. [53] and combined with the tool mr [83] which performs an OS-$\overline{\text{MS}}$ conversion and RGE running of all SM parameters incorporating all state-of-the-art higher-order corrections [84–89] (see also [90–93], where the OS-$\overline{\text{MS}}$ conversion formulae for the SM Higgs, top Yukawa, and gauge couplings have been computed at $\mathcal{O}(\alpha\alpha_s)$). In contrast, NMSSMCALC implements only the full one-loop and leading two-loop corrections in the extraction of the SM $\overline{\text{MS}}$ parameters. Therefore, we implemented an optional link of NMSSMCALC to the program mr which replaces the in-house calculations performed in steps 1a) to 3) in Fig. 1 with the predictions of mr. This ensures that we use the very same running SM $\overline{\text{MS}}$ parameters as Ref. [53] at a given scale Q_{match} for a given set of SM input parameters. Alternatively, we provide a similar link to the tool SMDR [94] which uses a different treatment of the Higgs tadpole and works in the $\overline{\text{MS}}$ scheme but goes similarly beyond the corrections computed by NMSSMCALC [95–102]. It should be noted that both, mr and SMDR, increase the runtime of NMSSMCALC significantly such that their use within a parameter scan effectively becomes unviable. However, in [103], the authors provide interpolation formulae based on SMDR covering a 5σ range of the SM input parameters. We implemented these interpolation formulae in NMSSMCALC as an alternative approach to extract the SM $\overline{\text{MS}}$ parameters, see Appendix B.

In Fig. 4 (left) we show the Higgs mass prediction applying the quartic coupling matching for M_h^{IV} for the parameter point BP1 as a function of λ. The parameter $\kappa = \lambda$ is varied simultaneously. The brown-solid line is a reprint the one-loop curve found in Ref. [53] (Fig. 1) while the orange-dashed, green-dotted and blue-solid lines are obtained with NMSSMCALC when using mr, SMDR or the in-built SM calculation, respectively. The blue band shows the uncertainty estimate (*cf.* Sect. 3.3) of the pure NMSSMCALC result as defined in Eq. (3.47). In the lower panel we plot the difference $\Delta = M_h^{\text{IV}}\big|_{\text{[53]}} - M_h^{\text{IV}}\big|_{\text{NMSSMCALC}}$ for each indi-

Table 4 Individual (first five columns) and total (last two columns) uncertainty estimate of the SM-like Higgs boson mass prediction for the three parameter points defined in Table 1. All values are given in units of MeV. The uncertainty $\Delta^{\text{SUSY}}_{v^2/M^2_{\text{SUSY}}}$ only contributes to the total uncertainty of the quartic coupling matching, i.e. to ΔM_h^{IV}

	$\Delta^{\text{SM}}_{Y_t}$	$\Delta^{\text{SM}}_{Q_{\text{EW}}}$	$\Delta^{\text{SM}}_{G_F/\alpha_{M_Z}}$	$\Delta^{\text{SUSY}}_{Q_{\text{match}}}$	$\Delta^{\text{SUSY}}_{v^2/M^2_{\text{SUSY}}}$	ΔM_h^{II}	ΔM_h^{IV}
BP1	−738	208	−19	376	−21	854	836
BP2	−685	208	−69	189	−5	743	743
BP3	−401	198	20	694	−2294	826	2415

vidual NMSSMCALC result. We find very good agreement between NMSSMCALC and Ref. [53] within the numerical accuracy if mr is used for the SM calculation (orange-dashed) which is a strong numerical cross-check of our quartic coupling matching. If we use SMDR instead of mr, the Higgs mass prediction is moved downwards by $\sim 100\,\text{MeV}$. The NMSSMCALC result differs by $\sim 500 - 600\,\text{MeV}$ throughout the shown range of λ but is in agreement with the other three results within the estimated uncertainty. Since the SM RGEs in NMSSMCALC are of the same order as in mr (full two-loop and leading three- and four-loop), the difference between the NMSSMCALC and mr result is mainly caused by missing higher-order corrections in the OS $-$ $\overline{\text{MS}}$ conversion performed by NMSSMCALC.

Furthermore, the availability of the pole-mass matching also enables us to perform another cross-check. The pole-mass and quartic-coupling matching only differ by terms of $\mathcal{O}(v^2/M^2_{\text{SUSY}})$ and consequently should converge to each other for large M_{SUSY} if all large logs appearing in the pole-mass calculation are cancelled properly. The two parameter points BP1 and BP2 are suitable for such a comparison as the BSM particle spectrum is of the order of the TeV-scale. In particular the stop masses, which control the numerically largest loop corrections, are above 2.5 TeV and hence the related uncertainties $\Delta^{\text{SUSY}}_{v^2/M^2_{\text{SUSY}}} \sim \mathcal{O}(10\,\text{Mev})$ (*cf.* Table 4). This behaviour is demonstrated in Fig. 4 (right) for the parameter point BP2 where all SUSY particle masses are varied simultaneously with M_{SUSY}. The blue-solid line shows the Higgs mass prediction obtained using the quartic-coupling matching, M_h^{IV}, while the red-dashed lines shows the result when using the pole-mass matching, M_h^{II}. In addition, we show the fixed-order result (black-solid) obtained in the $\overline{\text{DR}}$ scheme at $\mathcal{O}(\alpha_t(\alpha_t + \alpha_s))$.[19] The lower panel in Fig. 4 (right) shows the difference $\Delta = M_h^{\text{IV}} - M_h^i$ between the quartic coupling matching and the other two results. For large M_{SUSY}, starting from $M_{\text{SUSY}} > 2\,\text{TeV}$, we find perfect agreement between the pole-mass and quartic-coupling matching while for low M_{SUSY} they can differ by several GeV. The blue uncertainty-band for M_h^{IV} also includes the differences to the pole-mass matching result, thereby demonstrating the importance of the v^2/M^2_{SUSY} corrections in this regime. On the other hand, the fixed-order result and the pole-mass matching show better agreement for small M_{SUSY} while for larger M_{SUSY} the fixed-order line features a different shape. One might naively expect better agreement between the result obtained in the pole-mass matching and the fixed-order calculation if $M_{\text{SUSY}} < 1\,\text{TeV}$ (see e.g. [8]). However, the two-loop corrections to the matching condition taken from the literature do not contain any v^2/M^2_{SUSY} terms while the two-loop fixed-order calculation has the full dependence on the electroweak VEV. Thus, the discrepancy between the two approaches for very small M_{SUSY} can be explained by the missing v^2/M^2_{SUSY}-terms in the two-loop part of the EFT calculation. Indeed we verified numerically, that the fixed-order and EFT-pole-mass predictions agree better at low scales if only one-loop corrections are taken into account. Therefore, the pole-mass matching procedure implemented in NMSSMCALC possesses features of a hybrid approach taking into account resummed logs as well as pieces of v^2/M^2_{SUSY} as the *hybrid* approaches in FlexibleEFTHiggs [49–51,104] and FeynHiggs [3,105–108]. This method gives precise predictions for M_h across a large range of M_{SUSY} (see [8] for a complete list of references). However, parameter points like BP2 which are rather MSSM-like, often can only pass experimental constraints from stop searches, as well as the theoretical constraint of predicting $M_h \approx 125\,\text{GeV}$, by having M_{SUSY} larger than a few TeV and are therefore often saturated in the energy regime where a quartic coupling matching is sufficient. In the next section we show that this is not the case for the NMSSM, as it can predict a light singlet, which can greatly benefit from a pole-mass matching.

[19] Since BP2 is in the MSSM limit, this is the most precise 2-loop order available in NMSSMCALC.

4.4 The case of a light singlet

We now consider the scenario of a rather light singlet which is realised by the parameter point BP3. Note that due to the appearance of a light state, we do not expect the SM to be the correct EFT parametrisation for this parameter point (and instead, the SM extended by a singlet scalar should be used), but we nonetheless want to study its features and compare how well the two matching approaches perform. In Fig. 5 (left) we show the Higgs boson mass prediction using the quartic-coupling matching (blue-solid),

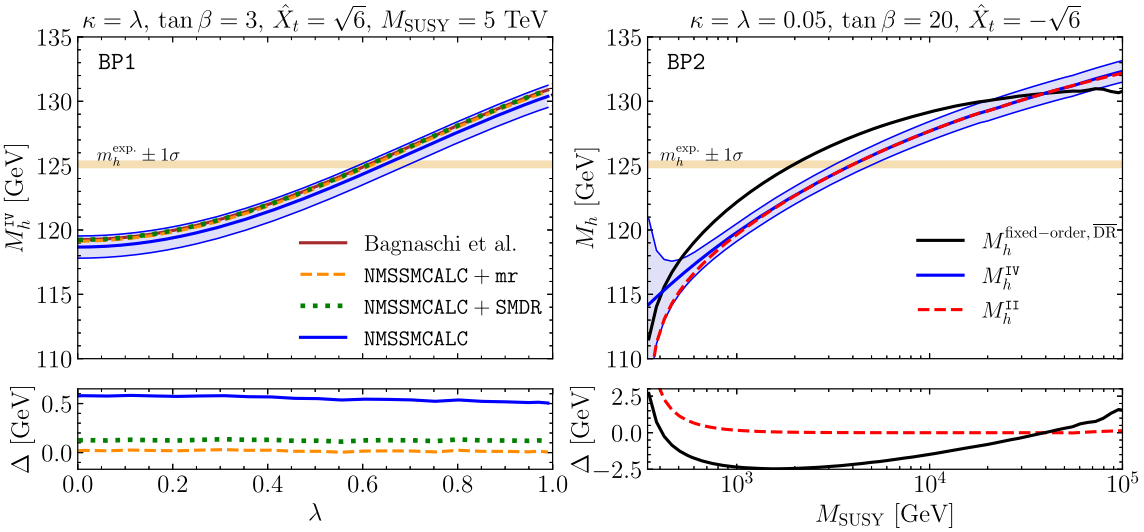

Fig. 4 Left: Higgs mass prediction for the parameter point BP1 as a function of λ using the quartic coupling matching. Shown are the results for $M_h^{\rm IV}$ and its uncertainty estimate defined in Eq. (3.47), obtained with NMSSMCALC (blue solid) or with a modified NMSSMCALC which uses mr (orange dashed) or SMDR (green dotted) for the SM OS-$\overline{\rm MS}$ conversion and SM RGE-running. In brown we re-print the result taken from Fig. 1 of Ref. [53]. The lower panel shows the differences of the result found in Ref. [53] and the results obtained with NMSSMCALC. Right: Higgs mass prediction for BP2 using the fixed-order (black), quartic coupling matching (blue), pole-mass matching (red dashed) calculation of NMSSMCALC. The blue band is the uncertainty of the quartic-coupling matching defined in Eq. (3.47). The lower panel shows the differences with the result obtained in the quartic-coupling matching

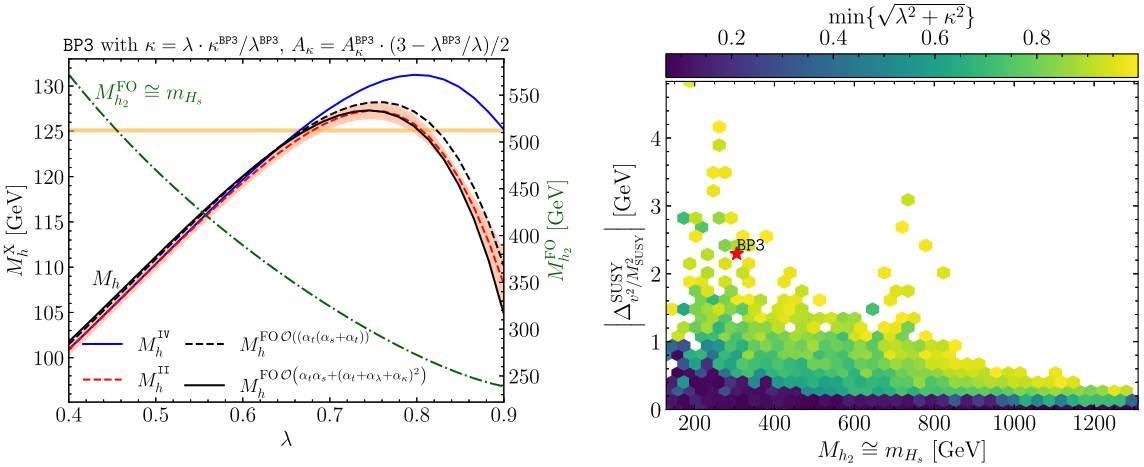

Fig. 5 Left: The SM-like Higgs boson mass computed using the quartic-coupling matching (blue), pole-mass matching (red dashed), fixed-order $\mathcal{O}(\alpha_t(\alpha_t+\alpha_s))$ (black dashed) and the fixed-order $\mathcal{O}(\alpha_t\alpha_s + (\alpha_t+\alpha_\lambda+\alpha_\kappa)^2)$ (black solid) calculation as a function of λ for the parameter point BP3. The green line (to be read on the right axis), shows the mass-prediction of the singlet-like state obtained at fixed order $\mathcal{O}\alpha_t\alpha_s + (\alpha_t+\alpha_\lambda+\alpha_\kappa)^2$. The red band is the uncertainty obtained for the pole-mass matching result, as defined in Eq. (3.46). Right: Size of the $v^2/M_{\rm SUSY}^2$-type corrections as a function of the second-lightest Higgs mass for all parameter points with a h_2 featuring at least 50% singlet admixture obtained in the random scan. Each hexagonal bin shows the minimum value of $\sqrt{\lambda^2+\kappa^2}$ found in that bin

the pole-mass matching approach (red-dashed, including the red uncertainty band, applying Eq. (3.46)) and the fixed-order calculation at $\mathcal{O}(\alpha_t(\alpha_t+\alpha_s))$ (black dashed) and $\mathcal{O}(\alpha_t\alpha_s + (\alpha_t+\alpha_\lambda+\alpha_\kappa)^2)$ (black solid) as a function of λ. The green line (to be read on the right axis) shows the fixed-order prediction for the mass m_{H_s} of the singlet-like state. We scale the other NMSSM-parameters according to $\kappa = \lambda \cdot \kappa^{\rm BP3}/\lambda^{\rm BP3}$, $A_\kappa = A_\kappa^{\rm BP3} \cdot (3 - \lambda^{\rm BP3}/\lambda)/2$. This parametrisation allows us to vary λ throughout a large range while maintaining a decreasing singlet mass with increasing λ and it furthermore avoids the presence of tachyonic tree-level masses. For $\lambda = \lambda^{\rm BP3}$ we recover the original parameter point. For small $\lambda \approx 0.4$ the singlet-like mass is about 500 GeV while for large $\lambda \approx 0.9$ it can be as light

as 250 GeV. The SM-Higgs boson mass varies between 100 and 131 GeV within the considered λ range. In the small-λ (and large m_{H_s}) region we observe good agreement between all four methods. However, as λ increases (m_{H_s} decreases) the quartic-coupling matching result starts to deviate, reaching a difference w.r.t. the other results of up to $\sim$ 15 GeV. It should be stressed that the stop masses are always above 1.5 TeV for this parameter point. Therefore, all v^2/M^2_{SUSY} contributions from the stop sector are negligible compared to those originating in the singlet sector.

It remains the question whether missing higher-order corrections to the matching condition proportional to λ and κ can become significant for large λ. While the two-loop corrections of this type to the matching condition are not available in NMSSMCALC, they, however, have been included in the NMSSMCALC fixed-order prediction [33]. This allows us to estimate the importance of NMSSM-specific corrections by comparing the three results. In Fig. 5 (left) we observe, that the relative size of the NMSSM-specific higher-order corrections in the fixed-order calculation is always much smaller than the relative size of the missing v^2/M^2_{SUSY} contributions in the EFT-approach. Therefore, the v^2/M^2_{SUSY} corrections in the one-loop matching condition of the quartic-coupling approach are numerically more significant than the missing NMSSM-specific higher-order corrections to the matching condition. Regarding the pole-mass matching the evaluation of the importance of the missing two-loop corrections is left for future work.

The region in Fig. 5 (left) that features very large $\Delta^{\text{SUSY}}_{v^2/M^2_{\text{SUSY}}}$ is clearly not in agreement with the Higgs boson mass measurement. It is interesting to ask how large $\Delta^{\text{SUSY}}_{v^2/M^2_{\text{SUSY}}}$ can be for parameter points satisfying the constraint. In Fig. 5 (right) we therefore study the size of the v^2/M^2_{SUSY} terms by plotting the absolute value of $\Delta^{\text{SUSY}}_{v^2/M^2_{\text{SUSY}}}$ for all parameter points found in the random scan, which fulfill all applied constraints and feature a second-lightest singlet-like scalar, as a function of the singlet mass m_{H_s}. The parameter points are grouped in hexagonal bins whereas the color of each bin indicates the minimum value of $\sqrt{\lambda^2+\kappa^2}$ found in that bin. We observe that $\Delta^{\text{SUSY}}_{v^2/M^2_{\text{SUSY}}}$ tends to decrease for increasing m_{H_s} and therefore shows a similar behaviour as the stop sector (note that e.g. the neutralinos could still be lighter than the singlet and also cause v^2/M^2_{SUSY} contributions). However, the size of $\Delta^{\text{SUSY}}_{v^2/M^2_{\text{SUSY}}}$ is also strongly influenced by the size of λ and κ. For $\sqrt{\lambda^2+\kappa^2} \lesssim 0.2$ we find $\Delta^{\text{SUSY}}_{v^2/M^2_{\text{SUSY}}} \lesssim 1$ GeV which is similar to what we obtain in the MSSM with the present exclusion limits on the stops. It is remarkable that the two matching approaches agree with each other reasonably well for small λ and κ even if the singlet is as light as 200 GeV (*cf.* dark blue points in the plot). However, for $\sqrt{\lambda^2+\kappa^2} \gtrsim 0.3$ the quartic-coupling matching would suffer from large missing v^2/M^2_{SUSY} corrections, which can reach up to $\mathcal{O}(5\,\text{GeV})$ for $\sqrt{\lambda^2+\kappa^2} \gtrsim 0.9$.

4.5 CP-violating effects in the EFT calculations

In the following we study the effect of non-vanishing CP-violating phases onto the Higgs mass prediction at the example of the parameter points BP1 and BP3. We distinguish two scenarios: (i) CP in the Higgs sector is conserved at the tree-level but broken by loop effects from the SUSY fermions and scalars and (ii) CP is already broken at the tree-level.

4.5.1 Loop-induced CP-violation

In Fig. 6 we show the Higgs mass prediction for BP1 (left) and BP3 (right) for individually varied phases of M_1 (blue), M_2 (black) and A_t (red). The lower panels show the prediction for the electric dipole moment of the electron (eEDM) obtained with NMSSMCALC normalised to the current experimental upper bound [109]. The solid lines show the Higgs mass prediction obtained with the pole-mass matching while the dashed lines are obtained with the quartic-coupling matching. In addition, the results of the quartic-coupling matching have been shifted by the constant difference $\Delta^{\text{SUSY}}_{v^2/M^2_{\text{SUSY}}}\Big|_{\varphi_i=0}$ from Table 4 such that the dashed and solid lines overlap for $\varphi = 0$. Therefore, one can directly read-off additional v^2/M^2_{SUSY}-effects caused by the CP-violating phases. For both parameter points we find that φ_{A_t} is not constrained by the eEDM while still having an effect on M_h of $\mathcal{O}(1\,\text{GeV})$. The phases $\varphi_{M_{1,2}}$ can have a similar effect on M_h but are strongly constrained when varied individually. It should be noted, however, that for some choices of $\varphi_{M_1} \neq \varphi_{M_2} \neq 0$ the EDM constraints can be avoided while still achieving non-negligible effects on M_h.

The v^2/M^2_{SUSY} effects caused by the CP-violating phases are negligible for the parameter point BP1 since all SUSY particles are heavy in this scenario. This is not the case for BP3, which has a rather light Higgsino and a large mixing between wino and Higgsino, and therefore a large $\Delta^{\text{SUSY}}_{v^2/M^2_{\text{SUSY}}}\Big|_{\varphi_{M_2}\neq 0}$ contribution.

4.5.2 Tree-level CP-violation

Considering Eq. (3.13c) any phase-combination $\varphi_y = 2\varphi_s + \varphi_\kappa - \varphi_\lambda - \varphi_u \neq 0$ will immediately introduce CP-violating effects in the Higgs sector thereby having a strong impact on the EDM prediction. In the following we focus on φ_λ and φ_κ which were found to have the smallest impact on the eEDM for the considered parameter points.

In Fig. 7 we show the same quantities as in Fig. 6 but as a function of φ_κ (red) and φ_λ (blue). We find that for

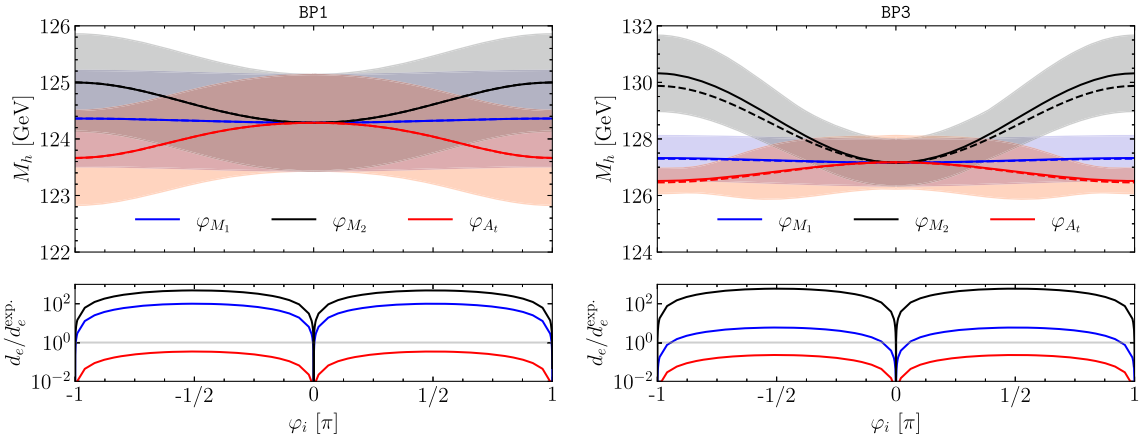

Fig. 6 The dependence of the Higgs mass prediction using the pole-mass matching (solid) and quartic-coupling matching (dashed) on the CP-violating phases of M_1 (blue), M_2 (black) and A_t (red). The quartic-coupling matching results have been shifted by the constant values $\Delta^{\text{SUSY}}_{v^2/M^2_{\text{SUSY}}}\Big|_{\varphi_i=0}$ from Table 4. Note that the phases in the plots are defined relative to the phases, i.e. signs, of the CP-conserving reference points, such that the benchmark scenarios in Table 1 are recovered for $\varphi_i = 0$

BP1 $|\varphi_\lambda| \gtrsim 0.05$ ($|\varphi_\kappa| \gtrsim 0.15$) and for BP3 $|\varphi_\lambda| \gtrsim 0.01$ ($|\varphi_\kappa| \gtrsim 0.03$) is excluded by the eEDM. However, even in these small ranges the Higgs mass prediction depends strongly on the CP-violating phases. Concerning the size of the v^2/M^2_{SUSY} contributions, the picture is similar to the loop-induced CP-case i.e. only BP3 shows a significant difference between pole-mass and quartic-coupling matching.

As an additional cross-check we verified that pole-mass and quartic-coupling matching (i.e. solid and dashed lines of the same color) are in agreement for all values considered in Figs. 6 and 7 once we set the running VEV $v(Q_{\text{match}})$ at the matching scale to a numerically small value in the pole-mass matching which effectively turns-off all v^2/M^2_{SUSY} corrections. However, for very large values of $|\lambda|$, $|\kappa|$ and $\varphi_y \sim \mathcal{O}(1)$ one may loop-induce sizeable mixing between CP-even and CP-odd Higgs fields (such that the SM is no longer the right EFT) even for $v \to 0$. Thus, CP-violating cases with very large CP-even/odd mixing have to be considered with caution. The matching to appropriate EFTs that are not the SM but include more light degrees of freedom is left for future work.

5 Conclusions

In this paper, we presented our new computation of the higher-order corrections to the SM-like Higgs boson of the CP-violating NSSM for large mass hierarchies. In this case, fixed-order computations become unreliable due to the involved logarithms of large mass hierarchies, requiring the application of an EFT framework. We chose a scenario where all non-SM particles are very heavy, so that the low-energy EFT is given by the SM. The matching of the full NMSSM to the SM at the high-scale is performed at full one-loop order in the NMSSM, including two-loop corrections in the MSSM limit. We applied two matching approaches given by the quartic coupling matching in the unbroken theory and the pole mass matching after EWSB. The latter includes terms of the order v^2/M^2_{SUSY}, so that the comparison between the two methods allowed us to estimate the importance of these terms that are neglected in the former approach. We additionally provided an estimate of the different sources of uncertainty. Our new computation has been implemented in the public program package NMSSMCALC and can be downloaded from the url:

https://www.itp.kit.edu/~maggie/NMSSMCALC/

For our numerical analysis, we performed a scan in the NMSSM parameter space and only kept points that are in agreement with the Higgs signal data and exclusion constraints on additional Higgs bosons and supersymmetric particles. We validated our calculation and implementation of the two matching procedures in NMSSMCALC against existing results in the literature and found good agreement for the tested parameter point. We subsequently investigated the case of a light singlet-like Higgs boson in the NMSSM spectrum. As expected, the EFT approach applying the pole-mass matching shows good agreement with the fixed-order result (including partly resummation in the top/stop sector by applying $\overline{\text{DR}}$ renormalisation [32]) within the theoretical uncertainty, while the quartic coupling matching starts more and more deviating with decreasing singlet mass due to the missing $\mathcal{O}(v^2/M^2_{\text{SUSY}})$ terms. The behavior is confirmed by the analysis of our entire found parameter sample. With increasing values of the specific NMSSM coupling parame-

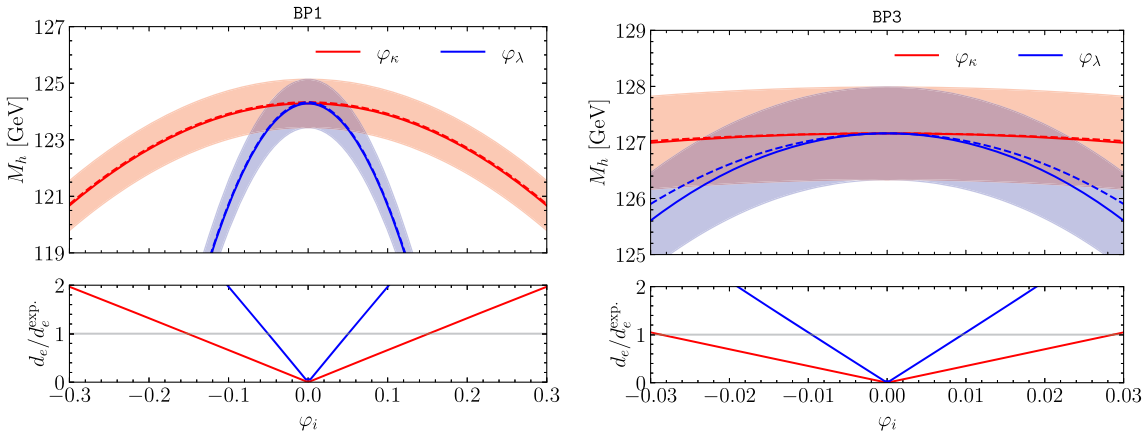

Fig. 7 The dependence of the Higgs mass prediction using the pole-mass matching (solid) and quartic-coupling matching (dashed) on the CP-violating phases of λ (blue) and κ (red). The quartic-coupling matching results have been shifted by the constant values $\Delta^{\text{SUSY}}_{v^2/M^2_{\text{SUSY}}}\Big|_{\varphi_i=0}$ from Table 4

ters λ and κ, the singlet-like Higgs boson mass decreases, and the v^2/M^2_{SUSY} effects beome increasingly important, deteriorating the description by the quartic coupling matching. Within the uncertainty band of the pole-mass matching, the two matching approached nevertheless can agree with each other even if the singlet mass is as light as 200 GeV provided that $\sqrt{\lambda^2+\kappa^2} \lesssim 0.2$. We studied for the first time the effects of CP violation in the EFT approach in the NMSSM. From a conceptual point of view, we found that care has to be taken in the derivation of the quartic-coupling matching in order not to miss finite contributions that do not appear in the CP-conserving case nor the CP-violating MSSM. This requires the expansion of the tadpoles up to $\mathcal{O}(v \times M^2_{\text{SUSY}})$. Both for loop-induced and tree-level CP violation, we find the v^2/M^2_{SUSY} contributions to the matching condition to become important for our benchmark point `BP3` which features a light singlet Higgs boson.

In summary, we find good agreement between the pole-mass and the quartic-coupling matching approaches within theoretical uncertainties and our EFT implementation reliably describes NMSSM scenarios with a heavy non-SM mass spectrum. Scenarios with light singlet-like states (i.e. lighter than 125 GeV) require the extension of the approach beyond the SM as effective low-energy description. This is left for future work.

Acknowledgements We thank Dominik Stöckinger and Johannes Wünsche for discovering a bug in the first release of the code that affected the implementation of the two-loop $\alpha_t(\alpha_s+\alpha_t)$ results for the matching condition from the literature.

Funding The research of C.B. and M.M. was supported by the Deutsche Forschungsgemeinschaft (DFG, German Research Foundation) under grant 396021762 - TRR 257. T.N.D thanks Phenikaa University for its financial support of this work. M.G. acknowledges support by the Deutsche Forschungsgemeinschaft (DFG, German Research Foundation) under Germany's Excellence Strategy - EXC 2121 "Quantum Universe" - 390833306 and partially by 491245950. H.R.'s research is funded by the Deutsche Forschungsgemeinschaft (DFG, German Research Foundation) - project no. 442089526.

Data Availability Statement This manuscript has no associated data. [Author's comment: Data sharing not applicable to this article as no datasets were generated or analysed during the current study].

Code Availability Statement Code/software will be made available on reasonable request. [Author's comment: The code/software generated during and/or analysed during the current study is available from the corresponding author on reasonable request.].

A Expansion of the one-loop tadpoles to $\mathcal{O}(v)$

In this appendix we derive the leading terms of $\delta^{(1)}t_{a_d}/v$ which are not suppressed by inverse powers of M_{SUSY}. The tadpole counterterm $\delta^{(1)}t_{a_d}$ can be expanded to $\mathcal{O}(v \times M^2_{\text{SUSY}})$ in two equivalent ways. The first method involves considerations about the dependence of couplings, mixing matrices and mass eigenvalues on the SM VEV. The second method relies on a systematic expansion in v.

Method (i): The couplings entering the Feynman diagrams of $\delta^{(1)}t_{a_d}$ in general consist of a linear combination of v-independent factors, which correspond to couplings defined in the gauge-basis (or unbroken EW phase) and of v-dependent mixing-matrices. The lowest dependence of the mass eigenvalues on v is of $\mathcal{O}(v^2)$ in the tadpole diagrams. The only linear dependence on v arises in the mixing matrices that hence need to be expanded to $\mathcal{O}(v)$. The expansion of the mixing matrices can be performed by using the solutions of the rotation matrices that have been obtained analytically for the case $v = 0$ as an ansatz and introducing $\mathcal{O}(v)$-terms on the off-diagonal elements. These elements can be determined by requiring unitarity of the mixing matrix up to $\mathcal{O}(v^2/M^2_{\text{SUSY}})$ and by requiring that the mass matrix with the full v-dependence is diagonalised up to $\mathcal{O}(v^2/M^2_{\text{SUSY}})$. For the example of the stop-mixing matrix $\tilde{U}$ we find at $\mathcal{O}(v/M_{\text{SUSY}})$:

$$\tilde{U}_{ii} = 1,$$
$$\tilde{U}_{12} = -\left(\tilde{U}_{21}\right)^* = \frac{v}{2}\frac{\sqrt{2}e^{i(\varphi_w-\varphi_y+\varphi_{A_t})}|A_t| - |\lambda|v_s\cot\beta}{m^2_{\tilde{Q}_3} - m^2_{\tilde{U}_{R,3}}} e^{\varphi_\lambda+\varphi_s},$$

whereas the squared mass-eigenvalues do not receive additional corrections at $\mathcal{O}(v/M_{\text{SUSY}})$ but only at $\mathcal{O}(v^2/M^2_{\text{SUSY}})$. The resulting stop-contribution to the counterterm reads

$$\delta^{(1)}t_{a_d} = v\frac{3|\lambda||A_t|v_s Y_t^2}{16\pi^2\sqrt{2}\sin\beta} B(m_{\tilde{Q}_3}, m_{\tilde{U}_{R,3}})\sin(\varphi_w - \varphi_y + \varphi_{A_t}), \tag{A.1}$$

with

$$B(x,y) = \frac{A(x)-A(y)}{x^2-y^2},$$
$$B(x,x) = \ln\frac{\mu^2}{x^2},$$
$$A(x) = x^2\left(1+\ln\frac{\mu^2}{x^2}\right),$$
$$A(0) = 0.$$

Method (ii): A systematic way of computing the tadpole without performing an explicit expansion of mixing matrix elements can be performed by considering the Taylor expansion of the tadpole counter-term around $v = 0$:

$$\delta^{(1)}t_{a_d} = v\cdot\left.\frac{\partial t_{a_d}}{\partial v}\right|_{v=0} + \mathcal{O}(v^2). \tag{A.2}$$

The tadpole itself can be written as the derivative of the one-loop effective potential $V^{(1)}$ w.r.t. the field a_d, i.e. $\delta^{(1)}t_{a_d} = \partial V^{(1)}/\partial a_d$. The derivative of the potential w.r.t. the SM-like Higgs VEV v can be replaced by the derivative w.r.t. the Higgs field itself. Thus, we find

$$\delta^{(1)}t_{a_d} = v\cdot\left.\frac{\partial^2 V(h,a_d,\dots)}{\partial a_d\partial h}\right|_{h=a_d=0;v=0} + \mathcal{O}(v^2) \tag{A.3a}$$
$$= v\cdot\Sigma_{h\to a_d}(p^2=0)\Big|_{v=0} + \mathcal{O}(v^2) \tag{A.3b}$$
$$= v\cdot\left(-\cos\beta\,\Sigma_{h\to G}(p^2=0) + \sin\beta\,\Sigma_{h\to A}(p^2=0)\right)\Big|_{v=0} + \mathcal{O}(v^2), \tag{A.3c}$$

where in the second line we used that the second derivative of the effective potential is equivalent to the self-energy evaluated at vanishing external momentum. In the last line we rotated the second index of the $i \to j$ self-energy from the gauge-basis into the mass-basis using Eq. (2.10). Note that the self-energy is again computed in the unbroken phase and can be conveniently generated with e.g. SARAH. Using this result we find full agreement with the stop contribution derived above. Furthermore, we also computed the full result including contributions from electroweakinos as well as the neutral and charged Higgses and found full agreement (within the numerical accuracy) with the result obtained when evaluating $\delta^{(1)}t_{a_d}/v$ numerically for $v = 1\,\text{GeV}$.

B New implementation in NMSSMCALC

In this appendix we describe how the new and old Higgs mass prediction in NMSSMCALC is controlled using the SLHA interface, and discuss examples of in- and output files.

The SLHA NMSSM input parameters are interpreted as $\overline{\text{DR}}$ parameters at the scale $Q_{\text{inp.}}$ (cf. Fig. 1 box 1b)). The fixed-order calculation implemented in NMSSMCALC allows to renormalise the charged Higgs boson mass $m^{\text{OS}}_{H^\pm}$ on-shell or to alternatively compute the charged Higgs boson mass at two-loop order and use $\text{Re}A_\lambda^{\overline{\text{DR}}}$ as input. Furthermore, NMSSMCALC has two options for the renormalisation scheme for the top/stop sector: on-shell and $\overline{\text{DR}}$. In contrast, the newly implemented EFT calculation currently only takes SUSY contributions in the $\overline{\text{DR}}$ scheme into account. Thus, we recommend to use the $\overline{\text{DR}}$ scheme in combination with the EFT calculation. However, it is in principle still possible to choose a different (the OS) scheme in the precision fixed-order prediction of the BSM masses by using the flags 7 and 8 in the MODSEL block, *cf.* Fig. 8. With flag 6, the user chooses the loop-order of the fixed-order calculation. These flags only concern the fixed-order calculations which are written out into the MASS block. In addition, there are three new flags, 15, 16 and 17, to control the calculation of the SM-like Higgs boson mass. If the EFT calculation was chosen by setting the flag 15 to a value larger than 10, the entry of the SM-like Higgs boson mass is overwritten with the EFT result while all other MASS entries are those obtained with the fixed-order

```
Block MODSEL
 3  1   # NMSSM
 5  2   # 0:CP-conserving; 2:general CP-violation
 6  3   # loop level of fixed-order calculations:
        #  1:one-loop; 2:O(αtαs); 3:O(αtαs + αt^2);
        #  4:O(αtαs + (αt + αλ + ακ)^2)
 7  2   # top/stop sector (in fixed-order calculation):
        #  2:DR; 3:OS scheme
 8  0   # 0:MHpm as OS-input; 1:ReAlambda as DR-input
 10 0   # EDM calculation:0/1/2 (off/on/detailed output)
 11 0   # AtextcolorredM calculation:0/1/2 (off/on/detailed
output)
 12 0   # compute effective HHH couplings:0/1 (off/on)
 13 0   # loop-corrected W-mass:0/1 (off/on)
 15 14  # fixed-order or EFT.
        #  -2:automatic; -1:always fixed-order;
        #  1n/2n:EFT with pole-mass/quartic matching
        #        at n-order with n=1:one-loop (this work);
        #        n=2:O(αsαt) [68]; n=3:O(αt^2) [68];
        #        n=4:O(αsαEW) [69]
 16 22  # extraction of MS SM parameters using
        #  αMZ-scheme (12) or GF-scheme (22),
        #  SMDR interpolation formulae [103] (49)
 17 1   # uncertainty estimate:0/1 (off/on)
```

Fig. 8 Example of all new and old flags available in the MODSEL-block of the SLHA input-file

```
BLOCK DMASS # Theoreticalerror
  25  9.52016291E-01 # H1
  35  3.00000000E+00 # H2
  36  3.00000000E+00 # H3
  45  3.00000000E+00 # H4
  46  3.00000000E+00 # H5
  37  3.00000000E+00 # Hc
 251 -8.17298889E-01 # Mh(Qmatch = Qinp) − Mh(Qmatch = Qinp/2)
 252  8.38518143E-01 # Mh(Qmatch = Qinp) − Mh(Qmatch = 2Qinp)
 253 -4.01258469E-01 # Δ^SM_Yt = Mh(Yt^SM,O(αs^3)) − Mh(Yt^SM,O(αs^2))
 254  2.09808350E-02 # Δ^SM_GF/αMZ = M_h^GF − M_h^αMZ
 255 -2.29334831E+00 # estimated size of v^2/MSUSY^2 terms (Δ^SUSY_v^2/MSUSY^2)
 256 -7.32089989E-02 # M_h^EFT − M_h^fixed-order (not included in total uncertainty)
 257  2.04386369E-01 # SM scale uncertainty (Δ^SM_QEW)
```

Fig. 9 Example of the DMASS block in the SLHA output-file. The numerical values correspond to the output obtained for the benchmark point BP3 using the pole-mass matching (MODSEL 15=14) and the G_F-scheme (MODSEL 16=22)

calculation (flags 6, 7, 8). For scenarios, where the SM-like Higgs is the lightest of the neutral Higgs bosons, this would be the entry of "MASS 25". If, however, the dominantly h_u-like Higgs boson is not the lightest neutral Higgs boson, the entry of the heavier neutral Higgs state corresponding to the SM-like Higgs is overwritten with the EFT result. In this case, however, the EFT approach is not valid any more as it assumes all other Higgs bosons to be heavy. The NMHMIXC block, containing the numerical values of the neutral Higgs mixing matrix, corresponds to the matrix that diagonalises the loop-corrected mass matrix if the fixed-order calculation was chosen by the user. If the EFT calculation is chosen, NMHMIXC corresponds to the tree-level mixing matrix. Setting flag 15 to -2, the program decides whether the fixed-order or the EFT calculation is performed, for scenarios where the size of the SUSY input scale (given in "EXTPAR 0") is larger than 1.5 TeV.[20] The input scale, if not specified by the user, by default is set to $Q_{\text{inp}} = \sqrt{m_{\tilde{Q}_3} m_{\tilde{u}_{R_3}}}$, which indicates the size of the stop masses. Scenarios with e.g. a light singlet,

[20] Note that the applied criterion is only a rough estimator for the validity of the EFT/fixed-order calculation.

where the EFT approach might be questionable, are therefore not recognised by this estimate. If flag 15 is set to -1, the program always uses the fixed-order rather than the EFT calculation. For flag 15 being between 11 and 24, the first digit (1 or 2) determines the EFT approach (pole-mass or quartic-coupling matching) and the second digit turns on various higher-order corrections in the EFT calculation, *cf.* Fig. 8. These are the full NMSSM one-loop corrections including CP-violating effects computed in this work and the 2-loop corrections in the MSSM limit at $\mathcal{O}(\alpha_s\alpha_t)$ with full mass dependence [68], $\mathcal{O}(\alpha_t^2)$ in the case of degenerate masses [68], and $\mathcal{O}(\alpha_s\alpha_{\rm EW})$ [69]. Setting flag 16 to 12 or 22 chooses the α_{M_Z} or the G_F-scheme in the extraction of the SM $\overline{\rm MS}$ parameters. Alternatively, we implemented the `SMDR` interpolation formulae [103] for the extraction of the SM $\overline{\rm MS}$ parameters as discussed in Sect. 4.3, which can be enabled by setting flag 16 to 49. Flag 17 controls the uncertainty estimate of the EFT calculation. In Fig. 9 we show the new `DMASS` block, which contains the theoretical uncertainty of the EFT result, obtained for the parameter point `BP3` with the settings given in Fig. 8. In addition to the total uncertainty ("`DMASS 25`", corresponding to Eq. (3.46)), it also lists the individual uncertainties as well as the difference to the fixed-order result obtained with the `MODSEL` flags 6, 7 and 8. The mass uncertainty of the BSM Higgs masses is set to the commonly chosen fixed value of 3 GeV. This is often larger than the overall size of the loop-corrections to the scalar BSM masses and therefore a rather conservative estimate.

References

1. ATLAS Collaboration collaboration, Observation of a new particle in the search for the Standard Model Higgs boson with the ATLAS detector at the LHC. Phys. Lett. B **716**, 1 (2012). https://doi.org/10.1016/j.physletb.2012.08.020. arXiv:1207.7214
2. CMS Collaboration collaboration, Observation of a new boson at a mass of 125 GeV with the CMS experiment at the LHC. Phys. Lett. B **716**, 30 (2012). https://doi.org/10.1016/j.physletb.2012.08.021. arXiv:1207.7235
3. T. Hahn, S. Heinemeyer, W. Hollik, H. Rzehak, G. Weiglein, High-precision predictions for the light CP – even Higgs boson mass of the minimal supersymmetric Standard Model. Phys. Rev. Lett. **112**, 141801 (2014). https://doi.org/10.1103/PhysRevLett.112.141801. arXiv:1312.4937
4. J.R. Ellis, J. Gunion, H.E. Haber, L. Roszkowski, F. Zwirner, Higgs Bosons in a nonminimal supersymmetric model. Phys. Rev. D **39**, 844 (1989). https://doi.org/10.1103/PhysRevD.39.844
5. M. Drees, Supersymmetric Models with extended Higgs sector. Int. J. Mod. Phys. A **4**, 3635 (1989). https://doi.org/10.1142/S0217751X89001448
6. U. Ellwanger, C. Hugonie, A.M. Teixeira, The next-to-minimal supersymmetric Standard Model. Phys. Rep. **496**, 1 (2010). https://doi.org/10.1016/j.physrep.2010.07.001. arXiv:0910.1785
7. M. Maniatis, The next-to-minimal supersymmetric extension of the Standard Model reviewed. Int. J. Mod. Phys. A **25**, 3505 (2010). https://doi.org/10.1142/S0217751X10049827. arXiv:0906.0777
8. P. Slavich, S. Heinemeyer et al., Higgs-mass predictions in the MSSM and beyond. Eur. Phys. J. C **81**, 450 (2021). https://doi.org/10.1140/epjc/s10052-021-09198-2. arXiv:2012.15629
9. U. Ellwanger, Radiative corrections to the neutral Higgs spectrum in supersymmetry with a gauge singlet. Phys. Lett. B **303**, 271 (1993). https://doi.org/10.1016/0370-2693(93)91431-L. arXiv:hep-ph/9302224
10. T. Elliott, S. King, P. White, Supersymmetric Higgs bosons at the limit. Phys. Lett. B **305**, 71 (1993). https://doi.org/10.1016/0370-2693(93)91107-X. arXiv:hep-ph/9302202
11. T. Elliott, S. King, P. White, Squark contributions to Higgs boson masses in the next-to-minimal supersymmetric standard model. Phys. Lett. B **314**, 56 (1993). https://doi.org/10.1016/0370-2693(93)91321-D. arXiv:hep-ph/9305282
12. T. Elliott, S. King, P. White, Radiative corrections to Higgs boson masses in the next-to-minimal supersymmetric Standard Model. Phys. Rev. D **49**, 2435 (1994). https://doi.org/10.1103/PhysRevD.49.2435. arXiv:hep-ph/9308309
13. P. Pandita, One loop radiative corrections to the lightest Higgs scalar mass in nonminimal supersymmetric Standard Model. Phys. Lett. B **318**, 338 (1993). https://doi.org/10.1016/0370-2693(93)90137-7
14. P. Pandita, Radiative corrections to the scalar Higgs masses in a nonminimal supersymmetric Standard Model. Z. Phys. C **59**, 575 (1993). https://doi.org/10.1007/BF01562550
15. S. King, P. White, Resolving the constrained minimal and next-to-minimal supersymmetric standard models. Phys. Rev. D **52**, 4183 (1995). https://doi.org/10.1103/PhysRevD.52.4183. arXiv:hep-ph/9505326
16. U. Ellwanger, C. Hugonie, Yukawa induced radiative corrections to the lightest Higgs boson mass in the NMSSM. Phys. Lett. B **623**, 93 (2005). https://doi.org/10.1016/j.physletb.2005.07.039. arXiv:hep-ph/0504269
17. G. Degrassi, P. Slavich, On the radiative corrections to the neutral Higgs boson masses in the NMSSM. Nucl. Phys. B **825**, 119 (2010). https://doi.org/10.1016/j.nuclphysb.2009.09.018. arXiv:0907.4682
18. F. Staub, W. Porod, B. Herrmann, The electroweak sector of the NMSSM at the one-loop level. JHEP **1010**, 040 (2010). https://doi.org/10.1007/JHEP10(2010)040
19. P. Drechsel, L. Galeta, S. Heinemeyer, G. Weiglein, Precise predictions for the Higgs-Boson masses in the NMSSM. Eur. Phys. J. C **77**, 42 (2017). https://doi.org/10.1140/epjc/s10052-017-4595-1
20. S. Ham, J. Kim, S. Oh, D. Son, The charged Higgs boson in the next-to-minimal supersymmetric standard model with explicit CP violation. Phys. Rev. D **64**, 035007 (2001). https://doi.org/10.1103/PhysRevD.64.035007. arXiv:hep-ph/0104144
21. S. Ham, S. Oh, D. Son, Neutral Higgs sector of the next-to-minimal supersymmetric standard model with explicit CP violation. Phys. Rev. D **65**, 075004 (2002). https://doi.org/10.1103/PhysRevD.65.075004. arXiv:hep-ph/0110052
22. S. Ham, Y. Jeong, S. Oh, Radiative CP violation in the Higgs sector of the next-to-minimal supersymmetric model. arXiv: hep-ph/0308264
23. K. Funakubo, S. Tao, The Higgs sector in the next-to-MSSM. Prog. Theor. Phys. **113**, 821 (2005). https://doi.org/10.1143/PTP.113.821. arXiv:hep-ph/0409294
24. S. Ham, S. Kim, S. Oh, D. Son, Higgs bosons of the NMSSM with explicit CP violation at the ILC. Phys. Rev. D **76**, 115013 (2007). https://doi.org/10.1103/PhysRevD.76.115013. arXiv:0708.2755
25. K. Cheung, T.-J. Hou, J.S. Lee, E. Senaha, The Higgs boson sector of the next-to-MSSM with CP violation. Phys. Rev.

D **82**, 075007 (2010). https://doi.org/10.1103/PhysRevD.82.075007. arXiv:1006.1458
26. M.D. Goodsell, F. Staub, The Higgs mass in the CP violating MSSM, NMSSM, and beyond. Eur. Phys. J. C **77**, 46 (2017). https://doi.org/10.1140/epjc/s10052-016-4495-9
27. F. Domingo, P. Drechsel, S. Paßehr, On-shell neutral Higgs bosons in the NMSSM with complex parameters. Eur. Phys. J. C **77**, 562 (2017). https://doi.org/10.1140/epjc/s10052-017-5104-2. arXiv:1706.00437
28. M.D. Goodsell, K. Nickel, F. Staub, Two-loop corrections to the Higgs masses in the NMSSM. Phys. Rev. D **91**, 035021 (2015). https://doi.org/10.1103/PhysRevD.91.035021
29. K. Ender, T. Graf, M. Muhlleitner, H. Rzehak, Analysis of the NMSSM Higgs Boson masses at one-loop level. Phys. Rev. D **85**, 075024 (2012). https://doi.org/10.1103/PhysRevD.85.075024
30. T. Graf, R. Grober, M. Muhlleitner, H. Rzehak, K. Walz, Higgs Boson masses in the complex NMSSM at one-loop level. JHEP **10**, 122 (2012). https://doi.org/10.1007/JHEP10(2012)122
31. M. Mühlleitner, D.T. Nhung, H. Rzehak, K. Walz, Two-loop contributions of the order $\mathcal{O}(\alpha_t\alpha_s)$ to the masses of the Higgs bosons in the CP-violating NMSSM. JHEP **05**, 128 (2015). https://doi.org/10.1007/JHEP05(2015)128. arXiv:1412.0918
32. T.N. Dao, R. Gröber, M. Krause, M. Mühlleitner, H. Rzehak, Two-loop $\mathcal{O}(\alpha_t^2)$ corrections to the neutral Higgs boson masses in the CP-violating NMSSM. JHEP **08**, 114 (2019). https://doi.org/10.1007/JHEP08(2019)114. arXiv:1903.11358
33. T.N. Dao, M. Gabelmann, M. Mühlleitner, H. Rzehak, Two-loop $\mathcal{O}((\alpha_t+\alpha_\lambda+\alpha_\kappa)^2)$ corrections to the Higgs boson masses in the CP-violating NMSSM. JHEP **09**, 193 (2021). https://doi.org/10.1007/JHEP09(2021)193. arXiv:2106.06990
34. J. Baglio, R. Grober, M. Muhlleitner, D. Nhung, H. Rzehak et al., NMSSMCALC: a program package for the calculation of loop-corrected Higgs boson masses and decay widths in the (complex) NMSSM. Comput. Phys. Commun. **185**, 3372 (2014). https://doi.org/10.1016/j.cpc.2014.08.005. arXiv:1312.4788
35. D.T. Nhung, M. Muhlleitner, J. Streicher, K. Walz, Higher order corrections to the trilinear Higgs self-couplings in the real NMSSM. JHEP **1311**, 181 (2013). https://doi.org/10.1007/JHEP11(2013)181. arXiv:1306.3926
36. M. Mühlleitner, D.T. Nhung, H. Ziesche, The order $\mathcal{O}(\alpha_t\alpha_s)$ corrections to the trilinear Higgs self-couplings in the complex NMSSM. JHEP **12**, 034 (2015). https://doi.org/10.1007/JHEP12(2015)034
37. C. Borschensky, T.N. Dao, M. Gabelmann, M. Mühlleitner, H. Rzehak, The trilinear Higgs self-couplings at $\mathcal{O}(\alpha_t^2)$ in the CP-violating NMSSM. Eur. Phys. J. C **83**, 118 (2023). https://doi.org/10.1140/epjc/s10052-023-11215-5. arXiv:2210.02104
38. T.N. Dao, M. Gabelmann, M. Mühlleitner, The $\mathcal{O}(\alpha_t+\alpha_\lambda+\alpha_\kappa)^2$ correction to the ρ parameter and its effect on the W boson mass calculation in the complex NMSSM. Eur. Phys. J. C **83**, 1079 (2023). https://doi.org/10.1140/epjc/s10052-023-12236-w. arXiv:2308.04059
39. U. Ellwanger, J.F. Gunion, C. Hugonie, NMHDECAY: a Fortran code for the Higgs masses, couplings and decay widths in the NMSSM. JHEP **02**, 066 (2005). https://doi.org/10.1088/1126-6708/2005/02/066. arXiv:hep-ph/0406215
40. U. Ellwanger, C. Hugonie, NMHDECAY 2.0: an updated program for sparticle masses, Higgs masses, couplings and decay widths in the NMSSM. Comput. Phys. Commun. **175**, 290 (2006). https://doi.org/10.1016/j.cpc.2006.04.004. arXiv:hep-ph/0508022
41. F. Staub, From superpotential to model files for FeynArts and CalcHep/CompHep. Comput. Phys. Commun. **181**, 1077 (2010). https://doi.org/10.1016/j.cpc.2010.01.011. arXiv:0909.2863
42. F. Staub, Automatic calculation of supersymmetric renormalization group equations and self energies. Comput. Phys. Commun. **182**, 808 (2011). https://doi.org/10.1016/j.cpc.2010.11.030. arXiv:1002.0840
43. F. Staub, SARAH 32: Dirac Gauginos, UFO output, and more. Comput. Phys. Commun. **184**, 1792 (2013). https://doi.org/10.1016/j.cpc.2013.02.019. arXiv:1207.0906
44. F. Staub, SARAH 4: a tool for (not only SUSY) model builders. Comput. Phys. Commun. **185**, 1773 (2014). https://doi.org/10.1016/j.cpc.2014.02.018. arXiv:1309.7223
45. W. Porod, SPheno, a program for calculating supersymmetric spectra, SUSY particle decays and SUSY particle production at e+ e- colliders. Comput. Phys. Commun. **153**, 275 (2003). https://doi.org/10.1016/S0010-4655(03)00222-4. arXiv:hep-ph/0301101
46. W. Porod, F. Staub, SPheno 31: extensions including flavour, CP-phases and models beyond the MSSM. Comput. Phys. Commun. **183**, 2458 (2012). https://doi.org/10.1016/j.cpc.2012.05.021. arXiv:1104.1573
47. B.C. Allanach, SOFTSUSY: a program for calculating supersymmetric spectra. Comput. Phys. Commun. **143**, 305 (2002). https://doi.org/10.1016/S0010-4655(01)00460-X. arXiv:hep-ph/0104145
48. B.C. Allanach, T. Cridge, The calculation of sparticle and Higgs decays in the minimal and next-to-minimal supersymmetric Standard Models: SOFTSUSY4.0. Comput. Phys. Commun. **220**, 417 (2017). https://doi.org/10.1016/j.cpc.2017.07.021. arXiv:1703.09717
49. P. Athron, J.-H. Park, D. Stöckinger, A. Voigt, FlexibleSUSY – a spectrum generator generator for supersymmetric models. Comput. Phys. Commun. **190**, 139 (2015). https://doi.org/10.1016/j.cpc.2014.12.020. arXiv:1406.2319
50. P. Athron, M. Bach, D. Harries, T. Kwasnitza, J.-H. Park, D. Stöckinger et al., FlexibleSUSY 2.0: extensions to investigate the phenomenology of SUSY and non-SUSY models. Comput. Phys. Commun. **230**, 145 (2018). https://doi.org/10.1016/j.cpc.2018.04.016. arXiv:1710.03760
51. P. Athron, J.-H. Park, T. Steudtner, D. Stöckinger, A. Voigt, Precise Higgs mass calculations in (non-)minimal supersymmetry at both high and low scales. JHEP **01**, 079 (2017). https://doi.org/10.1007/JHEP01(2017)079. arXiv:1609.00371
52. F. Staub, W. Porod, Improved predictions for intermediate and heavy supersymmetry in the MSSM and beyond. Eur. Phys. J. C **77**, 338 (2017). https://doi.org/10.1140/epjc/s10052-017-4893-7. arXiv:1703.03267
53. E. Bagnaschi, M. Goodsell, P. Slavich, Higgs-mass prediction in the NMSSM with heavy BSM particles. Eur. Phys. J. C **82**, 853 (2022). https://doi.org/10.1140/epjc/s10052-022-10810-2. arXiv:2206.04618
54. J. Baglio, T.N. Dao, M. Mühlleitner, One-loop corrections to the two-body decays of the neutral Higgs bosons in the complex NMSSM. Eur. Phys. J. C **80**, 960 (2020). https://doi.org/10.1140/epjc/s10052-020-08520-8. arXiv:1907.12060
55. E. Bagnaschi, G.F. Giudice, P. Slavich, A. Strumia, Higgs mass and unnatural supersymmetry. JHEP **09**, 092 (2014). https://doi.org/10.1007/JHEP09(2014)092. arXiv:1407.4081
56. H. Bahl, I. Sobolev, Two-loop matching of renormalizable operators: general considerations and applications. JHEP **03**, 286 (2021). https://doi.org/10.1007/JHEP03(2021)286. arXiv:2010.01989
57. D. Buttazzo, G. Degrassi, P.P. Giardino, G.F. Giudice, F. Sala, A. Salvio et al., Investigating the near-criticality of the Higgs boson. JHEP **12**, 089 (2013). https://doi.org/10.1007/JHEP12(2013)089. arXiv:1307.3536
58. I. Schienbein, F. Staub, T. Steudtner, K. Svirina, Revisiting RGEs for general gauge theories. Nucl. Phys. B **939**, 1 (2019). https://doi.org/10.1016/j.nuclphysb.2018.12.001. arXiv:1809.06797
59. K.G. Chetyrkin, M.F. Zoller, Three-loop \ beta-functions for top-Yukawa and the Higgs self-interaction in the Standard Model.

JHEP **06**, 033 (2012). https://doi.org/10.1007/JHEP06(2012)033. arXiv:1205.2892
60. K.G. Chetyrkin, M.F. Zoller, Leading QCD-induced four-loop contributions to the β-function of the Higgs self-coupling in the SM and vacuum stability. JHEP **06**, 175 (2016). https://doi.org/10.1007/JHEP06(2016)175. arXiv:1604.00853
61. S.P. Martin, M.T. Vaughn, Regularization dependence of running couplings in softly broken supersymmetry. Phys. Lett. B **318**, 331 (1993). https://doi.org/10.1016/0370-2693(93)90136-6. arXiv:hep-ph/9308222
62. J. Braathen, M.D. Goodsell, P. Slavich, Matching renormalisable couplings: simple schemes and a plot. Eur. Phys. J. C **79**, 669 (2019). https://doi.org/10.1140/epjc/s10052-019-7093-9. arXiv:1810.09388
63. M.E. Machacek, M.T. Vaughn, Two loop renormalization group equations in a general quantum field theory. 1. Wave function renormalization. Nucl. Phys. B **222**, 83 (1983). https://doi.org/10.1016/0550-3213(83)90610-7
64. M.E. Machacek, M.T. Vaughn, Two loop renormalization group equations in a general quantum field theory. 2. Yukawa couplings. Nucl. Phys. B **236**, 221 (1984). https://doi.org/10.1016/0550-3213(84)90533-9
65. M.E. Machacek, M.T. Vaughn, Two loop renormalization group equations in a general quantum field theory. 3. Scalar quartic couplings. Nucl. Phys. B **249**, 70 (1985). https://doi.org/10.1016/0550-3213(85)90040-9
66. M. Sperling, D. Stöckinger, A. Voigt, Renormalization of vacuum expectation values in spontaneously broken gauge theories. JHEP **07**, 132 (2013). https://doi.org/10.1007/JHEP07(2013)132. arXiv:1305.1548
67. M. Sperling, D. Stöckinger, A. Voigt, Renormalization of vacuum expectation values in spontaneously broken gauge theories: two-loop results. JHEP **01**, 068 (2014). https://doi.org/10.1007/JHEP01(2014)068. arXiv:1310.7629
68. J. Pardo Vega, G. Villadoro, SusyHD: Higgs mass determination in supersymmetry. JHEP **07**, 159 (2015). https://doi.org/10.1007/JHEP07(2015)159. arXiv:1504.05200
69. E. Bagnaschi, G. Degrassi, S. Paßehr, P. Slavich, Full two-loop QCD corrections to the Higgs mass in the MSSM with heavy superpartners. Eur. Phys. J. C **79**, 910 (2019). https://doi.org/10.1140/epjc/s10052-019-7417-9. arXiv:1908.01670
70. M. Gabelmann, M. Mühlleitner, F. Staub, Automatised matching between two scalar sectors at the one-loop level. Eur. Phys. J. C **79**, 163 (2019). https://doi.org/10.1140/epjc/s10052-019-6570-5. arXiv:1810.12326
71. J. Kublbeck, M. Bohm, A. Denner, Feyn arts: computer algebraic generation of Feynman graphs and amplitudes. Comput. Phys. Commun. **60**, 165 (1990). https://doi.org/10.1016/0010-4655(90)90001-H
72. T. Hahn, Generating Feynman diagrams and amplitudes with FeynArts 3. Comput. Phys. Commun. **140**, 418 (2001). https://doi.org/10.1016/S0010-4655(01)00290-9. arXiv:hep-ph/0012260
73. R. Mertig, M. Böhm, A. Denner, Feyn calc – computer-algebraic calculation of Feynman amplitudes. Comput. Phys. Commun. **64**, 345 (1991). https://doi.org/10.1016/0010-4655(91)90130-D
74. V. Shtabovenko, R. Mertig, F. Orellana, New developments in FeynCalc 9.0. Comput. Phys. Commun. **207**, 432 (2016). https://doi.org/10.1016/j.cpc.2016.06.008. arXiv:1601.01167
75. V. Shtabovenko, R. Mertig, F. Orellana, FeynCalc 9.3: new features and improvements. Comput. Phys. Commun. **256**, 107478 (2020). https://doi.org/10.1016/j.cpc.2020.107478. arXiv:2001.04407
76. T.N. Dao, L. Fritz, M. Krause, M. Mühlleitner, S. Patel, Gauge dependences of higher-order corrections to NMSSM Higgs boson masses and the charged Higgs decay $H^{\pm} \to W^{\pm} h_i$. Eur. Phys. J. C **80**, 292 (2020). https://doi.org/10.1140/epjc/s10052-020-7837-6. arXiv:1911.07197
77. F. Domingo, S. Paßehr, Towards Higgs masses and decay widths satisfying the symmetries in the (N)MSSM. Eur. Phys. J. C **80**, 1124 (2020). https://doi.org/10.1140/epjc/s10052-020-08655-8. arXiv:2007.11010
78. Particle Data Group Collaboration, Review of particle physics. *PTEP* **2022**, 083C01 (2022). https://doi.org/10.1093/ptep/ptac097
79. H. Bahl, T. Biekötter, S. Heinemeyer, C. Li, S. Paasch, G. Weiglein et al., HiggsTools: BSM scalar phenomenology with new versions of HiggsBounds and HiggsSignals. arXiv:2210.09332
80. P. Bechtle, D. Dercks, S. Heinemeyer, T. Klingl, T. Stefaniak, G. Weiglein et al., HiggsBounds-5: testing Higgs sectors in the LHC 13 TeV era. arXiv:2006.06007
81. P. Bechtle, S. Heinemeyer, T. Klingl, T. Stefaniak, G. Weiglein, J. Wittbrodt, HiggsSignals-2: probing new physics with precision Higgs measurements in the LHC 13 TeV era. Eur. Phys. J. C **81**, 145 (2021). https://doi.org/10.1140/epjc/s10052-021-08942-y. arXiv:2012.09197
82. M. Masip, R. Munoz-Tapia, A. Pomarol, Limits on the mass of the lightest Higgs in supersymmetric models. Phys. Rev. D **57**, R5340 (1998). https://doi.org/10.1103/PhysRevD.57.R5340. arXiv:hep-ph/9801437
83. B.A. Kniehl, A.F. Pikelner, O.L. Veretin, mr: a C++ library for the matching and running of the Standard Model parameters. Comput. Phys. Commun. **206**, 84 (2016). https://doi.org/10.1016/j.cpc.2016.04.017. arXiv:1601.08143
84. A.V. Bednyakov, A.F. Pikelner, V.N. Velizhanin, Anomalous dimensions of gauge fields and gauge coupling beta-functions in the Standard Model at three loops. JHEP **01**, 017 (2013). https://doi.org/10.1007/JHEP01(2013)017. arXiv:1210.6873
85. A.V. Bednyakov, A.F. Pikelner, V.N. Velizhanin, Yukawa coupling beta-functions in the Standard Model at three loops. Phys. Lett. B **722**, 336 (2013). https://doi.org/10.1016/j.physletb.2013.04.038. arXiv:1212.6829
86. A.V. Bednyakov, A.F. Pikelner, V.N. Velizhanin, Higgs self-coupling beta-function in the Standard Model at three loops. Nucl. Phys. B **875**, 552 (2013). https://doi.org/10.1016/j.nuclphysb.2013.07.015. arXiv:1303.4364
87. B.A. Kniehl, A.F. Pikelner, O.L. Veretin, Two-loop electroweak threshold corrections in the Standard Model. Nucl. Phys. B **896**, 19 (2015). https://doi.org/10.1016/j.nuclphysb.2015.04.010. arXiv:1503.02138
88. T. van Ritbergen, J.A.M. Vermaseren, S.A. Larin, The four loop beta function in quantum chromodynamics. Phys. Lett. B **400**, 379 (1997). https://doi.org/10.1016/S0370-2693(97)00370-5. arXiv:hep-ph/9701390
89. J.A.M. Vermaseren, S.A. Larin, T. van Ritbergen, The four loop quark mass anomalous dimension and the invariant quark mass. Phys. Lett. B **405**, 327 (1997). https://doi.org/10.1016/S0370-2693(97)00660-6. arXiv:hep-ph/9703284
90. F. Bezrukov, M.Y. Kalmykov, B.A. Kniehl, M. Shaposhnikov, Higgs boson mass and new physics. JHEP **10**, 140 (2012). https://doi.org/10.1007/JHEP10(2012)140. arXiv:1205.2893
91. F. Jegerlehner, M.Y. Kalmykov, O. Veretin, MS versus pole masses of gauge bosons: electroweak bosonic two loop corrections. Nucl. Phys. B **641**, 285 (2002). https://doi.org/10.1016/S0550-3213(02)00613-2. arXiv:hep-ph/0105304
92. F. Jegerlehner, M.Y. Kalmykov, O. Veretin, MS-bar versus pole masses of gauge bosons. 2. Two loop electroweak fermion corrections. Nucl. Phys. B **658**, 49 (2003). https://doi.org/10.1016/S0550-3213(03)00177-9. arXiv:hep-ph/0212319
93. F. Jegerlehner, M.Y. Kalmykov, O(alpha alpha(s)) correction to the pole mass of the t quark within the standard model. Nucl. Phys.

B **676**, 365 (2004). https://doi.org/10.1016/j.nuclphysb.2003.10.012. arXiv:hep-ph/0308216
94. S.P. Martin, D.G. Robertson, Standard model parameters in the tadpole-free pure $\overline{\rm MS}$ scheme. Phys. Rev. D **100**, 073004 (2019). https://doi.org/10.1103/PhysRevD.100.073004. arXiv:1907.02500
95. S.P. Martin, D.G. Robertson, TSIL: a program for the calculation of two-loop self-energy integrals. Comput. Phys. Commun. **174**, 133 (2006). https://doi.org/10.1016/j.cpc.2005.08.005. arXiv:hep-ph/0501132
96. S.P. Martin, D.G. Robertson, Higgs boson mass in the Standard Model at two-loop order and beyond. Phys. Rev. D **90**, 073010 (2014). https://doi.org/10.1103/PhysRevD.90.073010. arXiv:1407.4336
97. S.P. Martin, Pole mass of the W boson at two-loop order in the pure $\overline{MS}$ scheme. Phys. Rev. D **91**, 114003 (2015). https://doi.org/10.1103/PhysRevD.91.114003. arXiv:1503.03782
98. S.P. Martin, Z-boson pole mass at two-loop order in the pure $\overline{MS}$ scheme. Phys. Rev. D **92**, 014026 (2015). https://doi.org/10.1103/PhysRevD.92.014026. arXiv:1505.04833
99. S.P. Martin, Top-quark pole mass in the tadpole-free $\overline{MS}$ scheme. Phys. Rev. D **93**, 094017 (2016). https://doi.org/10.1103/PhysRevD.93.094017. arXiv:1604.01134
100. S.P. Martin, D.G. Robertson, Evaluation of the general 3-loop vacuum Feynman integral. Phys. Rev. D **95**, 016008 (2017). https://doi.org/10.1103/PhysRevD.95.016008. arXiv:1610.07720
101. S.P. Martin, Effective potential at three loops. Phys. Rev. D **96**, 096005 (2017). https://doi.org/10.1103/PhysRevD.96.096005. arXiv:1709.02397
102. S.P. Martin, Three-loop QCD corrections to the electroweak boson masses. Phys. Rev. D **106**, 013007 (2022). https://doi.org/10.1103/PhysRevD.106.013007. arXiv:2203.05042
103. Z. Alam, S.P. Martin, Standard model at 200 GeV. Phys. Rev. D **107**, 013010 (2023). https://doi.org/10.1103/PhysRevD.107.013010. arXiv:2211.08576
104. T. Kwasnitza, D. Stöckinger, A. Voigt, Improved MSSM Higgs mass calculation using the 3-loop FlexibleEFTHiggs approach including x_t-resummation. JHEP **07**, 197 (2020). https://doi.org/10.1007/JHEP06(2023)201. arXiv:2003.04639
105. H. Bahl, W. Hollik, Precise prediction for the light MSSM Higgs boson mass combining effective field theory and fixed-order calculations. Eur. Phys. J. C **76**, 499 (2016). https://doi.org/10.1140/epjc/s10052-016-4354-8. arXiv:1608.01880
106. H. Bahl, Pole mass determination in presence of heavy particles. JHEP **02**, 121 (2019). https://doi.org/10.1007/JHEP02(2019)121. arXiv:1812.06452
107. H. Bahl, S. Heinemeyer, W. Hollik, G. Weiglein, Theoretical uncertainties in the MSSM Higgs boson mass calculation. Eur. Phys. J. C **80**, 497 (2020). https://doi.org/10.1140/epjc/s10052-020-8079-3. arXiv:1912.04199
108. H. Bahl, S. Heinemeyer, W. Hollik, G. Weiglein, Reconciling EFT and hybrid calculations of the light MSSM Higgs-boson mass. Eur. Phys. J. C **78**, 57 (2018). https://doi.org/10.1140/epjc/s10052-018-5544-3. arXiv:1706.00346
109. ACME Collaboration, Improved limit on the electric dipole moment of the electron. Nature **562**, 355 (2018). https://doi.org/10.1038/s41586-018-0599-8